Environmental Chemistry and Ecotoxicology 7 (2025) 1370–1385

Contents lists available at ScienceDirect

Environmental Chemistry and Ecotoxicology

journal homepage: www.keaipublishing.com/en/journals/environmental-chemistry-and-ecotoxicology/

Research Paper

Foliar Fe_2O_3 nanoparticles enhance cadmium tolerance in *Amaranthus hypochondriacus* by modulating cell wall immobilization and antioxidant defenses

Yanfeng Hu [a], Jia You [b], Yue Xiang [a], Runze Tian [a], Jianli Wang [b], Zhongbao Shen [b], Yansheng Li [a,*]

[a] Northeast Institute of Geography and Agroecology, Chinese Academy of Sciences, Harbin, Heilongjiang 150081, China
[b] Institute of Pratacultural Science, Heilongjiang Academy of Agricultural Sciences, Harbin, Heilongjiang 150086, China

ARTICLE INFO

Keywords:
Cadmium
Phytoremediation
Nanoparticle
Reactive oxygen species
Cell wall

ABSTRACT

The integration of nanotechnology with high biomass plants offers a sustainable strategy for rehabilitating cadmium (Cd)-contaminated lands. However, the potential of iron-based nanoparticles (Fe-NPs) to enhance Cd phytoremediation in the hyperaccumulator *Amaranthus hypochondriacus* remains unclear. The current study demonstrates that foliar spraying of 100 mg L^{-1} Fe-NPs (α-Fe_2O_3) alleviated Cd (10 mg kg^{-1})-induced growth inhibition (plant height, leaf area, and biomass), and partially restored leaf photosynthetic parameters and chloroplast morphology. Fe-NPs also reduced Cd-triggered oxidative damage by decreasing reactive oxygen species (ROS) and malondialdehyde (MDA) levels while enhancing antioxidant activities in leaves. Moreover, Fe-NPs treatment significantly increased Cd accumulation in leaves and total Cd extraction, indicating enhanced phytoremediation efficiency. Meanwhile, Fe-NPs modified the subcellular Cd distribution in leaves, increasing cell wall Cd fixation from 56.8 % to 61.57 %. Transcriptomic analysis revealed that Fe-NPs + Cd treatment induced the most differentially expressed genes (1097 upregulated, 572 downregulated), mainly enriched in DNA-binding, protein catalysis, chloroplast function, cell wall dynamics, metal ion binding. Notably, Fe-NPs upregulated a group of wall-associated receptor-like kinase (*WAKL*) genes that were downregulated by Cd. Furthermore, *AhWAKL16* overexpression in hairy roots significantly increased cell wall Cd content by 14 % and mitigated Cd-induced root elongation inhibition and MDA accumulation. This work highlights the potential of Fe-NPs for Cd remediation in *A. hypochondriacus,* and provides the first evidence that Fe-NPs enhance Cd tolerance, at least partially, through *WAKL*-mediated Cd immobilization in the cell wall.

1. Introduction

Cadmium (Cd) pollution in agricultural soil, due to different human activities such as the use of agriculture fertilizers, industrial production, and urban waste, has inevitable drawn environmental concern [1]. Cd is a toxic and persistent heavy metal that readily accumulates in the inedible parts of plants, posing a severe threat to food safety and human health [2]. Cd is highly water-soluble and can be rapidly taken up by plant roots, subsequently translocated via the xylem to aerial parts, and redistributed from mature tissues to young tissues and seeds through the phloem [3]. Excessive accumulation of Cd in plants inhibits their growth and development by disrupting photosynthetic and respiratory systems, generating oxidative stress and lipid peroxidation, competing with the uptake and translocation of water and nutrient elements, and inhibiting antioxidant defenses [3]. Concurrently, plants have evolved a series of strategies to counteract Cd toxicity, including cell wall adsorption, cytoplasmic chelation, vacuolar sequestration, and storage in specific tissues [4].

Phytoremediation has emerged as an effective and environmentally friendly technology that utilizes hyperaccumulator or resistant plant species to extract metals from contaminated soils. Generally, the efficiency of Cd phytoremediation requires large plant biomass or high Cd concentrations, or both, in underground tissues. Currently, several plant species, such as *Phytolacca acinosa*, *Solanum nigrum*, *Solanum photeinocarpum*, *Sedum plumbizincicola*, and *Thlaspi caerulescens*, have been identified as Cd hyperaccumulators and exhibit tolerance to high Cd

* Corresponding author.
E-mail address: liyansheng@iga.ac.cn (Y. Li).

https://doi.org/10.1016/j.enceco.2025.06.015
Received 15 April 2025; Received in revised form 17 June 2025; Accepted 20 June 2025
Available online 21 June 2025

concentrations [5–7]. However, these hyperaccumulators, when grown in complex soil environments, have relatively slow growth rates and low biomass production, thus limiting their efficiency in phytoremediation in Cd-contaminated soils. Grain amaranth, *Amaranthus hypochondriacus* L., is an annual herbaceous plant primarily utilized as a grain crop and for fodder, medicinal, and ornamental purposes [8]. The use of *A. hypochondriacus* for Cd phytoremediation is increasingly attractive due to its fast growth, large biomass, and ability to thrive under diverse conditions [9]. For example, this species can absorb Cd in its leaves with a maximum concentration of 179.1 mg kg^{-1} [9], which exceeds the threshold value (100 mg kg^{-1}) of a Cd hyperaccumulator [10]. When Cd contamination level is above 75 mg kg^{-1} in soil, the highest Cd concentration in the shoots of *A. hypochondriacus* reaches 241.6 mg kg^{-1} [11], which is higher than that for other Cd hyperaccumulators, such as *S. photeinocarpum* (158 mg kg^{-1}) [7] and *Lantana camara* (139.7 mg kg^{-1}) [12]. In acidic soil, this plant is also tolerant to Cd toxicity and can extract more Cd (0.92 mg pot^{-1}) than other hyperaccumulators (*S. nigrum*, *P. acinosa*, and *S. plumbizincicola*) [6], suggesting its potential for Cd phytoextraction. Recently, *A. hypochondriacus* cultivar has also been used in rotation with winter rapeseed to improve the phytoextraction efficiency of Cd-contaminated farmland on the northern plains of China [13].

Cd phytoremediation in hyperaccumulator plants can be improved through the use of exogenous additives or agricultural technologies. For instance, researchers have shown that application of EDTA and organic acids increases the Cd availability in *Brassica juncea* from smelter-contaminated soils [14]. Exogenous silicon has been found to improve Cd accumulation in *Sedum alfredii* by enhancing Cd uptake [15]. Studies have also demonstrated that plant growth regulators, such as indole-3-acetic acid (IAA) and brassinosteroids (BR), can boost the phytoremediation efficiency of *S. alfredii* in contaminated soil by increasing biomass and Cd accumulation [16]. Other research indicated that plant growth-promoting rhizobacteria-assisted techniques can enhance the phytoextraction of Cd from polluted soils [17]. Similarly, several studies have reported the enhancement of *A. hypochondriacus* phytoextraction potential in Cd-contaminated soils through the utilization of antioxidants [18,19], plant hormones [20], microorganisms [21], and fertilizers [9].

Previous studies have indicated that the integration of nanotechnology into agricultural practices represents a promising strategy to improve crop yield, plant tolerance, and the phytoremediation efficiency of heavy metals [22]. Iron-based nanoparticles (Fe-NPs), such as Fe_2O_3, $Fe_7(PO_4)_6$, and Fe_3O_4, have been extensively used for in situ soil decontamination and boosting plant productivity due to their small size, large surface area, controlled release, and low toxicity [23,24]. Research has found that optimizing Fe-NPs application can produce multiple positive effects, including promoting plant growth and nutrient uptake [25], enhancing photosynthesis and antioxidant capacity under diverse abiotic stresses [26,27], and suppressing plant disease [28]. Most recently, a 4-year field study provided evidence that application of Fe-NP fertilizers can increase rice production and reduce emissions of methane (CH_4) and nitrous oxide (N_2O) in rice fields [29]. Nevertheless, little is known about the influence of Fe-NPs on Cd phytoremediation in *A. hypochondriacus* species.

Fe is an essential element for plant growth and development, playing an important role in various physiological processes, such as respiration, photosynthesis, and nitrogen assimilation and fixation [30]. Cd can disrupt Fe homeostasis in plants by interfering with its uptake from roots to shoots, thereby inducing Fe deficiency and impairing photosynthetic capacity [27,31]. Compared to other NPs (e.g., TiO_2, ZnO, SiO_2, CaO), Fe-NPs exhibit exceptional promise for agricultural applications, enhancing crop growth and Fe nutrient accumulation [26,32,33]. We therefore hypothesized that foliar application of Fe-NPs to *A. hypochondriacus* would improve Fe acquisition under Cd stress while enhancing Cd tolerance and extraction capacity. To test this, the current study used a red variety of *A. hypochondriacus* 'Longxian-1' (developed through inbreeding) to assess the effects of Fe-NPs on growth, Cd accumulation, subcellular distribution, leaf physiological changes, photosynthetic parameters, and transcriptomic characteristics under Cd stress. Additionally, to decipher the molecular mechanism of Cd tolerance, we cloned a cell wall-associated receptor-like kinase 16 (*AhWAKL16*) gene responsive to Fe-NPs and Cd treatments, and investigated its function in regulating Cd accumulation and tolerance in transgenic hairy roots. This study provides novel insights into the mechanisms by which Fe-NPs mitigate Cd toxicity in *A. hypochondriacus* and highlights their potential for improving phytoremediation efficiency in Cd-contaminated soils.

2. Materials and methods

2.1. Characterization of ferric oxide nanoparticles

The α-Fe_2O_3 NPs (claimed particle sizes of 20–30 nm and a purity of 99.0 %) used in this study were rust-brown powders, and purchased from Guangzhou Hongwu Materials Technology Co., Ltd. (https://www.hwnanomaterial.com). The size and morphology of the Fe-NPs were characterized using transmission electron microscopy (TEM, JEM-1200EX, Japan) and field emission scanning electron microscopy (SEM, Zeiss-Sigma300). The Fe-NPs consisted of rod-shaped particles, with measured sizes ranging from 22 nm to 61 nm (Supplementary Fig. 1A and B). The XRD spectrum of the Fe-NPs was assessed using an XRD-6100 X-ray diffractometer (Shimadzu, Japan), and is represented in Supplementary Fig. 1C. The zeta potential of Fe-NPs is 4.66 ± 0.84 mV at pH 7.0, as determined using the dynamic light scattering (Zetasizer Nano ZS90, Malvern Instrument, UK).

2.2. Plant materials and pot experiment design

A. hypochondriacus var. 'Longxian-1' was used in this study. 'Longxian-1' is a red variety bred by the Institute of Pratacultural Science, Heilongjiang Academy of Agricultural Sciences. This variety exhibits high seed yield and good quality in the field and better germination potential under Cd stress (Supplementary Fig. 2).

The pot experiment was conducted in a greenhouse under controlled conditions (14-h light/10-h dark photoperiod, temperature range of 21-28 °C, and relative humidity of 60 % - 80 %) in two periods. From August to September 2023, the effect and optimal concentration of Fe-NPs on *A. hypochondriacus* growth were determined in the pot experiment 1. Healthy seeds of *A. hypochondriacus* were surface-sterilized with a 2 % (*v*/v) sodium hypochlorite solution and sown in plastic boxes containing vermiculite as the germination substrate. Upon germination, seedlings were pre-cultivated in a plant growth chamber at 24/18 °C under a 16/8-h light/dark cycle before being transplanted into pots. Soil samples (from a depth of 0–20 cm) used for the pot assay were collected from the Minzhu experiment farmland of Heilongjiang Academy of Agricultural Science. The fundamental properties of the soil were as follows: organic carbon content, 134.61 g kg^{-1}; total nitrogen (N),1.57 g kg^{-1}; total phosphorus (P), 0.69 g kg^{-1}; total potassium (K), 16.22 g kg^{-1}; available N, 219.52 mg kg^{-1}; available P, 23.66 mg kg^{-1}; available K, 143.57 mg kg^{-1}; pH 6. 15. The soil samples were air-dried at room temperature, ground, and sieved through 2-mm meshes. At the two-leaf stage, uniform seedlings were selected and transplanted into plastic pots (5 cm × 7 cm × 10 cm, one seedling per pot filled with 0.5 kg of soil). For the Fe-NPs treatment, foliar spraying was chosen as a convenient and effective applied method based on previous studies [28,32]. Before application, the Fe-NPs were diluted in distilled water through sonication for 30 min. Total five Fe-NPs concentrations (0, 50, 100, 200, and 500 mg L^{-1}) were applied to seedlings of *A. hypochondriacus*. Ten milliliters of Fe-NPs solution was sprayed onto the leaves of each plant at four-day intervals (a total of three times), while an equal volume of distilled water was applied to the control (CK) group. During foliar application, the pots were covered with protective aluminum foil to prevent the Fe-NPs

entering the soil. After 14 days of Fe-NPs treatment, *A. hypochondriacus* plants were harvested to determine their dry weight and leaf cell viability.

Pot experiment 2 was conducted from May 2024 to October 2024 in the Institute of Pratacultural Science under the same greenhouse conditions. A concentration of 100 mg L^{-1} Fe-NPs spraying was found in pot experiment 1 to have a positive impact on the normal growth of *A. hypochondriacus* plants without causing obvious cytotoxicity to leaves (Supplementary Fig. 3). Therefore, four treatments were set up: application of 100 mg L^{-1} Fe-NPs, 10 mg kg^{-1} Cd plus 100 mg L^{-1} Fe-NPs, 10 mg kg^{-1} Cd treatment alone, and without Cd and Fe_2O_3-NPs as the control (CK). For the Cd treatment, the sieved soil was contaminated with a 100 mg L^{-1} $CdCl_2$·2.5 H_2O (Sigma) solution and then air-dried. The contaminated soil was thoroughly mixed with the remaining soil to achieve a Cd content of 10 mg kg^{-1}, and then placed in the dark for two weeks to stabilize the metal before cultivation. When *A. hypochondriacus* reached the two fully expanded leaves, uniform seedlings were divided into four groups and transplanted into plastic pots (13 cm × 17 cm × 19 cm, four seedlings per pot filled with 2 kg of soil) for individual and combined treatments of Cd and Fe-NPs. All pots were randomly arranged in the greenhouse and watered three times a week, with one application of a half-strength Hoagland nutrient solution. After 14 days of treatment, *A. hypochondriacus* plants were harvested to determine growth and physiological parameters, enzyme activities, element contents, and gene expression. To assess the impact of Fe-NPs on Cd extraction, pot soil and the remaining *A. hypochondriacus* plants were collected after 90 days of treatment for subsequent Cd content detection.

2.3. Analysis of leaf photosynthesis-related parameters

The analysis of changes in plant photosynthetic fluorescence was conducted using the PlantExplorer™ platform, which comprises an automated, high-resolution, multispectral camera system (PhenoVation, Netherlands). A minimum of twelve plants per treatment were imaged for fluorescence data collection. Quantification of leave photosynthetic parameters, including the maximum quantum efficiency of photosystem II (PSII) (F_v/F_m), the chlorophyll fluorescence index (ChIdx), and the anthocyanin index (AriIdx), was performed using the "Data Analysis Software" program (PhenoVation B.V., Wageningen, Netherlands) according to the manufacturer's instructions.

2.4. Transmission electron microscopy of leaf

Leaves were cut into small pieces of approximately 0.5 cm^2 and quickly immersed in 2.5 % glutaraldehyde (*v*/v) for 4 h at 4 °C. After washing in 0.1 M phosphate buffer (pH 7.2), the leaf tissues were fixed in 1 % osmium tetroxide for 2 h. Once fixed, the samples were dehydrated through a series of ethanol solutions (30 %, 50 %, 70 %, 90 %, and 100 %) and embedded in epoxy resin EPON 812 (Sigma). Ultrathin sections were prepared using an ultramicrotome Ultracut E (PC PowerTome, RMC Product, Tucson, AZ, USA). The sections were then examined and photographed with a transmission electron microscope JEM-1200EX (JEOL, Japan).

2.5. Determination of Cd and Fe contents

To analyze the contents of Cd and Fe in different plant tissues, 1.0 g of dried plant samples were ground and digested in a HNO_3: H_2O_2: HF (*v*/v/v = 5:2:0.7) solution using a microwave digestion system (JUPITER-B, Shanghai, China). The digested samples were transferred to volumetric flasks and adjusted to a total volume of 10 mL with 1 % HNO_3 (*v*/v). The contents of Cd and Fe were then measured using ICP-OES (Plasma Quant 9100, Jena, Germany). For soil Cd analysis, air-dried soil samples (0.25 g) were ground and then ashed with NaOH (2 g) in a muffle furnace. The mixture was first ashed at 400 °C for 15 min, followed by a second ashing at 720 °C for an additional 15 min. Total soil Cd was determined using ICP-OES.

2.6. Analysis of Cd subcellular distribution in A. hypochondriacus leaves

The Cd concentrations in subcellular components of *A. hypochondriacus* leaves were determined according to the methods previously described by Yang et al. [34]. Briefly, 1 g of fresh leaves were frozen in liquid nitrogen and ground in 10 mL of extraction buffer (50 mM Tris-HCl, 1 mM mercaptoethanol, 250 mM sucrose, pH 7.5). The homogenate was initially sieved through a nylon cloth with a 100 μm mesh size, and the residue was subsequently washed twice with extraction buffer. The collected washes, together with the initial filtrate, were then centrifuged at 1000 *g* for 20 min. The pellet, combined with the residue from the cloth filtration, formed the cell wall fraction (F_{cw}), which contained mainly cell walls and cell wall debris. The supernatant was then centrifuged again at 12,000 *g* for 45 min to obtain the cell organelle fraction (F_o). The remaining supernatant constituted the cell soluble fraction (F_s). Finally, the F_{cw} and F_o were dried at 70 °C and digested in a HNO_3: H_2O_2: HF solution to measure Cd contents, as described in the previous section. The F_s fraction was directly mixed with HNO_3 solution for digestion, and the Cd concentration was determined using ICP-OES.

2.7. Determination of malondialdehyde (MDA), cell viability, and reactive oxygen species (ROS) production

The MDA contents in leaf tissues were measured using an MDA Assay Kit (Beijing Boxbio Science Technology, Beijing, China) with a FlexA-200 Microplate Reader (ALLSHENG, Hangzhou, China) at wavelengths of 450 nm, 532 nm, and 600 nm. Evans blue staining was performed to detect leaf cells viability. Leaf samples were stained with 25 % (*w*/*v*) Evans blue solution for 20 min. After washing to remove excess dye, the leaves were homogenized, and the absorbance of released Evans blue was measured at 600 nm. The accumulation of H_2O_2 and O_2^- in leaves were detected by staining in 1 mg mL^{-1} diaminobenzidine (DAB) (Sigma) and a solution of 0.05 % (w/v) nitro blue tetrazolium (NBT), respectively. Then, leaves were observed and photographed for each treatment in each experiment. Additionally, the contents of H_2O_2 and O_2^- were quantified using a spectrophotometric method with commercial Plant ROS Assay Kits (Beijing Boxbio Science Technology, Beijing, China) according to the manufacturer's guidelines.

2.8. Detection of the reduced glutathione (GSH) and proline content and antioxidant enzyme activities

The contents of proline and reduced GSH in leaves were determined according to the commercial plant kits (Beijing Boxbio Science Technology, Beijing, China) following the manufacturers' instructions. The extraction and determination of antioxidant enzyme activities, including catalase (CAT), peroxidase (POD), superoxide dismutase (SOD), ascorbate peroxidase (APX), and glutathione reductase (GR), were conducted using commercial plant enzyme kits (Beijing Boxbio Science Technology, Beijing, China) following the manufacturers' instructions. All absorbance measurements were performed using the spectrophotometer.

2.9. RNA isolation, library construction and RNA-seq analysis

RNA-seq analysis was performed by LC-Bio Technology CO., Ltd. (Hangzhou, China). The *A. hypochondriacus* seedlings, at the two fully expanded-leaf stage, were treated with distilled water (CK), 10 mg kg^{-1} Cd, 100 mg L^{-1} Fe-NPs, and 10 mg kg^{-1} Cd plus 100 mg L^{-1} Fe-NPs for 14 days (treatment methodology followed Section 2.2). Each treatment included three biological samples. To form one biological replicate, leaves from four *A. hypochondriacus* plants were pooled. A total of twelve

leaf samples from *A. hypochondriacus* plants under CK, Cd, Fe-NP, and Fe-NP + Cd treatments were prepared for RNA isolation, library construction, and sequencing. Total RNA was extracted using TRIzol reagent (Invitrogen, Carlsbad, CA, USA). The amount and purity of RNA were determined using a NanoDrop ND-1000 (NanoDrop, Wilmington, DE, USA). RNA integrity was evaluated by 1.2 % denaturing agarose gel electrophoresis and further checked by a Bioanalyzer 2100 (Agilent, CA, USA). RNA samples with an RIN number > 7.0 were submitted to LC-Bio Technology CO., Ltd. for library construction and RNA sequencing on an Illumina Novaseq™ 6000 with 2 × 150 bp paired-end reads. Sequence quality was verified using the fastp software (https://github.com/OpenGene/fastp). High-quality reads from all samples were aligned to the reference genome of *A. hypochondriacus* v2.1 with HISAT2 (https://ccb.jhu.edu/software/hisat2). Differentially expressed genes (DEGs) were identified between the control and treated groups with a false discovery (FDR) < 0.05 and an absolute fold change ≥2. Functional analysis of the DEGs were carried out using Gene Ontology (GO) (http://geneontology.org/)) and Kyoto Encyclopedia of Genes and Genomes (KEGG) (http://www.genome.jp/kegg) pathways enrichment analysis tools.

2.10. Quantitative real time (qRT)-PCR analysis

Total RNA was isolated from *A. hypochondriacus* leaves and roots using the RNAPrep Pure Micro Kit (TianGen Biotech, Beijing, China) according to the manufacturer's instructions. One microgram (1 μg) of total RNA was used for first-strand cDNA synthesis with the RT SuperMix FastKing Kit (TianGen Biotech, Beijing, China). qRT-PCR assay was performed using the AceQ qPCR SYBR Green Master Mix kit (Vazyme, Nanjing, China) in the LightCycler® 480 System, following the manufacturer's procedure. The gene-specific primers used for the PCR reactions are listed in Supplementary Table 1. The data were compared using the mean Ct values of three biological replicates (each with three technical replicates) normalized to the mean Ct values of *AhActin* (the reference control gene). The relative expression levels of specific genes were calculated using the $2^{-\Delta\Delta Ct}$ method.

2.11. Plasmid construction and expression of AhWAKL16 in A. hypochondriacus hairy roots for functional analysis

To generate transgenic *A. hypochondriacus* hairy roots overexpressing *AhWAKL16*, the full-length coding region of *AhWAKL16* was cloned and inserted into the pCAMBIA1300-35S vector using specific primers (Supplementary Table 1). The pCAMBIA1300 vector contains the GFP gene as a selectable marker. All sequences were confirmed by sequencing. The transformation vector harboring *35S-AhWAKL16*, as well as the empty *pCAMBIA1300* vector, was introduced into *Agrobacterium rhizogenes* strain K599.

Transgenic *A. hypochondriacus* roots of composite plants were produced using a reliable and efficient *A. rhizogenes*-mediated transformation method for grain amaranth species [35], with minor modifications. 'LongXian-1' seeds were surface-sterilized with bleach. After germination on 1/2 MS medium plates, 12-day-old seedlings were excised at the hypocotyls using a sharp razor blade. The base of the excised seedlings was immediately submerged in K599 culture (OD_{600} = 0.4) for approximately 1 h. After co-cultivation, the plants were washed with sterile water to remove *A. rhizogenes*. The inoculated plants were then transferred to 1/2 MS medium containing timentin (300 mg L^{-1}, Sigma) and grown in a growth chamber. Approximately three weeks after inoculation, the transgenic hairy roots were screened using a fluorescent protein (GFP) excitation light source (Exc 440 nm, Em 500 nm, LUYOR-3415RG, China). Composite plants with GFP-expressing roots were used to assess Cd tolerance. In addition, transgenic hairy roots were also collected in three biological replicates for RNA extraction and qRT-PCR analysis of *AhWAKL16* expression levels. For Cd tolerance analysis, the selected positive composite plants were transferred to 1/2 MS medium plates with or without 50 μmol L^{-1} $CdCl_2$ for 7 days. Roots and leaves were collected for the analysis of growth and physiological parameters, as well as Cd content.

2.12. Statistical analysis

All data were subjected to analysis of variance (ANOVA) using SPSS Statistics 25.0 (IBM, Armonk, NY, USA). Significant differences between the control and treatment groups were determined using Tukey's Honestly Significant Difference (HSD) test at a significance level of $p < 0.05$. In all figures and tables, error bars represent the standard error (SE) of the group means. Each experiment was repeated at least three times.

3. Results

3.1. Effects of Fe-NPs application on A. hypochondriacus growth under Cd stress

The effect and optimal concentration of Fe-NPs on *A. hypochondriacus* growth were initially tested after foliar spray for 14 days. Fe-NPs at concentrations ranging from 50 to 200 mg L^{-1} did not significantly affect the biomass of *A. hypochondriacus*. Interestingly, 100 mg L^{-1} Fe-NPs showed a slight increase in plant dry weight, whereas 500 mg L^{-1} Fe-NPs significantly reduced the dry weight by 20.19 % (Supplementary Fig. 3A). Evans blue staining indicated that higher concentrations of Fe-NPs (200 and 500 mg L^{-1}) resulted in obvious leaf cell death and induced cytotoxicity in leaves of *A. hypochondriacus* plants (Supplementary Fig. 3B). Consequently, the application of 100 mg L^{-1} Fe-NPs was the safe concentration for *A. hypochondriacus* growth, and was used to further investigate the effect of Fe-NPs application on Cd tolerance in *A. hypochondriacus*. Compared to the CK group, *A. hypochondriacus* plants under 10 mg kg^{-1} Cd stress displayed notable growth inhibition, including leaf chlorosis, reduced plant height, and decreased leaf area (Fig. 1). However, the application of Fe-NPs improved the phenotype and plant biomass of *A. hypochondriacus* under Cd treatment, with the fresh weight, dry weight, and plant height increasing significantly by 34.99 %, 43.2 %, and 11.64 % ($p < 0.05$), respectively (Fig. 1). Moreover, the total leaf area reduction induced by Cd was nearly restored to CK levels following the application of Fe-NPs (Fig. 1). Likewise, Fe-NPs also mitigated the inhibitory effect of Cd on the growth of the *A. hypochondriacus* Reddish-green variety 'XCS' (Supplementary Fig. 4A), particularly when sprayed with 100 mg L^{-1} Fe-NPs. This treatment significantly increased plant dry weights, leaf length, and width by 41.1 %, 34.29 %, and 42.22 %, respectively, compared to those treated with Cd alone (Supplementary Fig. 4B and C).

3.2. Effects of Fe-NPs on plant photosynthesis and leaf structure of A. hypochondriacus under Cd stress

Spraying with Fe-NPs and exposure to Cd stress both resulted in noticeable changes in the maximum quantum yield of PSII (F_v/F_m), chlorophyll index (CHI), and anthocyanin index (ARI) of *A. hypochondriacus* leaves (Fig. 2A). Compared with the CK, Cd treatment caused a significant ($p < 0.05$) reduction in F_v/F_m by 3.16 % and an increase in non-photochemical quenching (NPQ) by 38.89 %. However, when Fe-NPs were applied to Cd-treated plants, these photosynthetic parameters were almost restored to CK levels (Fig. 2B). Furthermore, Fe-NPs also improved the vegetation indices ARI and CHI in *A. hypochondriacus* leaves under Cd stress (Fig. 2B). Similarly, application of Fe-NPs significantly increased the total chlorophyll content of leaves by 0.58 mg g^{-1} FW in Cd-treated plants compared to those Cd-treated alone (Supplementary Fig. 5). As shown in Fig. 2C, Cd treatment led to severely disorganized chloroplast structures and damage to the grana lamellae, resulting in an unstacked shape. The accumulation of starch grains in chloroplasts was also affected in Cd-treated *A. hypochondriacus* plants. However, the disruption of chloroplast

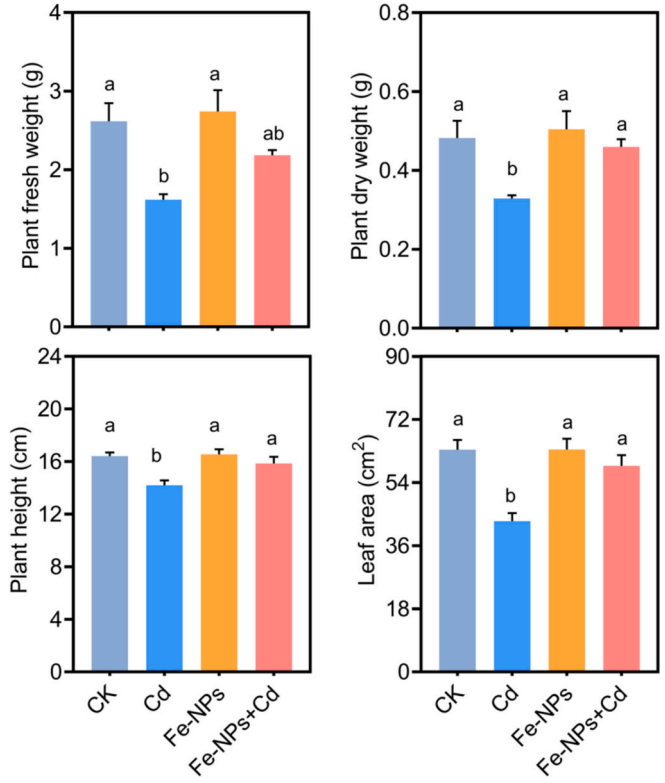

Fig. 1. Fresh weight, dry weight, height, and leaf area of *A. hypochondriacus* plants after 14 days treatment under four conditions: Cd (10 mg kg^{-1} $CdCl_2$), Fe-NPs (100 mg L^{-1}), Fe-NPs + Cd, and control (CK, without Cd and Fe-NPs). Values are means ± SE. Bar with different lowercase letters indicate significant differences between treatments according to one-way ANOVA and Turkey's tests ($p < 0.05$).

structures was less severe in Fe-NPs-sprayed plants under Cd stress (Fig. 2C). Notably, no significant changes in chloroplast structures were observed between the Fe-NPs-treated plants and the CK group.

3.3. Effects of Fe-NPs on ROS generation and antioxidant defense system of A. hypochondriacus leaves under Cd stress

Histochemical staining using DAB and NBT showed lower levels of ROS in CK and Fe-NPs treatment groups. In contrast, intense staining was observed on the surfaces of leaves in Cd-treated plants (Fig. 3A). Spraying Fe-NPs reduced ROS accumulation in *A. hypochondriacus* leaves induced by Cd (Fig. 3A). Specifically, the contents of H_2O_2 and O_2^- in leaves of the Fe-NPs + Cd group decreased significantly by 52.12 % and 26.96 % ($p < 0.05$) compared to Cd treatment alone, respectively (Fig. 3B). Consistent with the observed changes in ROS levels, lighter staining and significantly lower uptake of Evans blue were found in leaves of the Fe-NPs + Cd group (Fig. 3B), indicating alleviating effects of Fe-NPs on Cd-induced leaf cell death. MDA content, an indicator of membrane lipid peroxidation, was elevated by 79.51 % in Cd-treated leaves compared to the CK, but Fe-NPs treatment decreased MDA production under Cd stress (Fig. 3B). Moreover, the contents of proline and soluble sugars, which are major oxidative stress regulators, were significantly higher in leaves of Fe-NPs-treated plants compared to those exposed to Cd stress (Fig. 3B). Fe-NPs and Cd treatments also regulated the antioxidant defense system in the leaves of *A. hypochondriacus* in response to alterations in ROS levels. Compared to the CK, the activities of CAT and APX in the leaves under Cd stress were significantly decreased by 48.54 % and 41.48 %, respectively (Fig. 4), while application of Fe-NPs alone markedly increased the activity of SOD, CAT, and GR by 37.8 %, 48.28 %, and 253.21 %, respectively (Fig. 4). Notably, in comparison with Cd treatment alone, Fe-NPs restored the leaf CAT and POD activities under Cd treatment, increasing by 154.6 % and 201.11 % (Fig. 4). Additionally, the GSH content was higher in the leaves of Fe-NPs-treated plants than in the CK and Cd treatment groups (Fig. 4).

3.4. Effects of Fe-NPs on the concentrations of Cd and Fe in A. hypochondriacus

The Cd content in the roots of *A. hypochondriacus* plants, which were sprayed with Fe-NPs, was significantly reduced by 31.68 % compared to plants treated with Cd alone ($p < 0.05$). However, the application of Fe-NPs resulted in a significant increase in Cd content in leaves by 18.69 % (Fig. 5A). Cd treatment affected Fe uptake in the roots, causing a slight decrease of 12.02 % in Fe content. Nevertheless, the application of Fe-NPs increased the Fe content both in the roots and leaves by 18.28 % and 97.16 % (Fig. 5B), respectively, indicating effective alleviation of Cd-induced Fe deficiency in *A. hypochondriacus*. To assess the impact of Fe-NPs on the phytoremediation efficiency of *A. hypochondriacus,* the Cd extraction by plants per pot and soil Cd removal rate were determined after 90 days of the Fe-NPs treatment. In the Fe-NPs group, the extracted Cd amount of *A. hypochondriacus* plants was 909.5 μg per pot, which was 7.86 % higher than that in the Cd treatment alone (843.2 μg per pot). The Fe-NPs-treated plants in Cd-contaminated pot soil also had higher soil Cd removal rate (Supplementary Table 2). These findings suggest that Fe-NPs application increased the ability of *A. hypochondriacus* to extract Cd.

3.5. Effects of Fe-NPs on Cd subcellular distribution in A. hypochondriacus leaves

To further investigate the influence of Fe-NPs application on Cd distribution in leaves, the Cd content in the cell wall fraction (F_{cw}), organelle fraction (F_o), and soluble fraction (F_s) was analyzed. Fe-NPs significantly increased Cd content in the Fcw fraction, which was 1.28-fold higher compared to that in Cd-treated plants (Fig. 6A). In contrast, the Cd contents in the F_o and Fs fractions were not significantly affected by Fe-NPs (Fig. 6A). As shown in Fig. 6B, Cd is predominantly distributed in the cell wall fraction of *A. hypochondriacus* leaves. Under treatment with Fe-NPs, the proportion of Cd in the F_o decreased by 8.33 %, whereas the proportions of Cd in the F_s and F_{cw} increased by 3.56 % and 4.77 %, respectively, compared to the Cd-treated group. These results demonstrate that Fe-NPs application increases Cd accumulation in the cell wall of *A. hypochondriacus* leaves.

3.6. Effects of Fe-NPs on transcriptome profiling of A. hypochondriacus leaves under Cd stress

RNA-seq analysis indicated that Cd and Fe-NPs treatments markedly altered the transcriptome profiles of *A. hypochondriacus* leaves (Supplementary Fig. 6). A total of 235 DEGs (133 upregulated, 102 downregulated), 1182 DEGs (532 upregulated, 650 downregulated), 1669 DEGs (1097 upregulated, 572 downregulated), and 826 DEGs (703 upregulated, 123 downregulated) were identified in the comparisons of Fe-NPs_vs_CK, Cd_vs_CK, Fe-NPs + Cd_vs_CK, and Fe-NPs + Cd_vs_Cd, respectively (Fig. 7A and Supplementary Fig. 6). Notably, Fe-NPs alone induced the fewest DEGs, while the Fe-NPs + Cd treatment produced the highest number of DEGs, which suggested stronger gene regulation. In the Cd_vs_CK comparison, more DEGs were downregulated than those upregulated. Conversely, in the Fe-NPs + Cd_vs_CK and Fe-NPs + Cd_vs_Cd comparisons, a greater number of DEGs were upregulated than downregulated (Fig. 7A). To validate the accuracy of RNA-seq data, the expression levels of six randomly selected DEGs were analyzed by qRT-PCR (Supplementary Fig. 7). These genes included *AhWRKY70* (*AH021703*), *AhNHL3* (*AH021765*), *AhCIPK6* (*AH023489*), *AhCML18* (*AH022811*), *AhERF4* (*AH015249*), and *AhADH7* (*AH013384*). In agreement with the RNA-seq results (Supplementary Table 3), all six

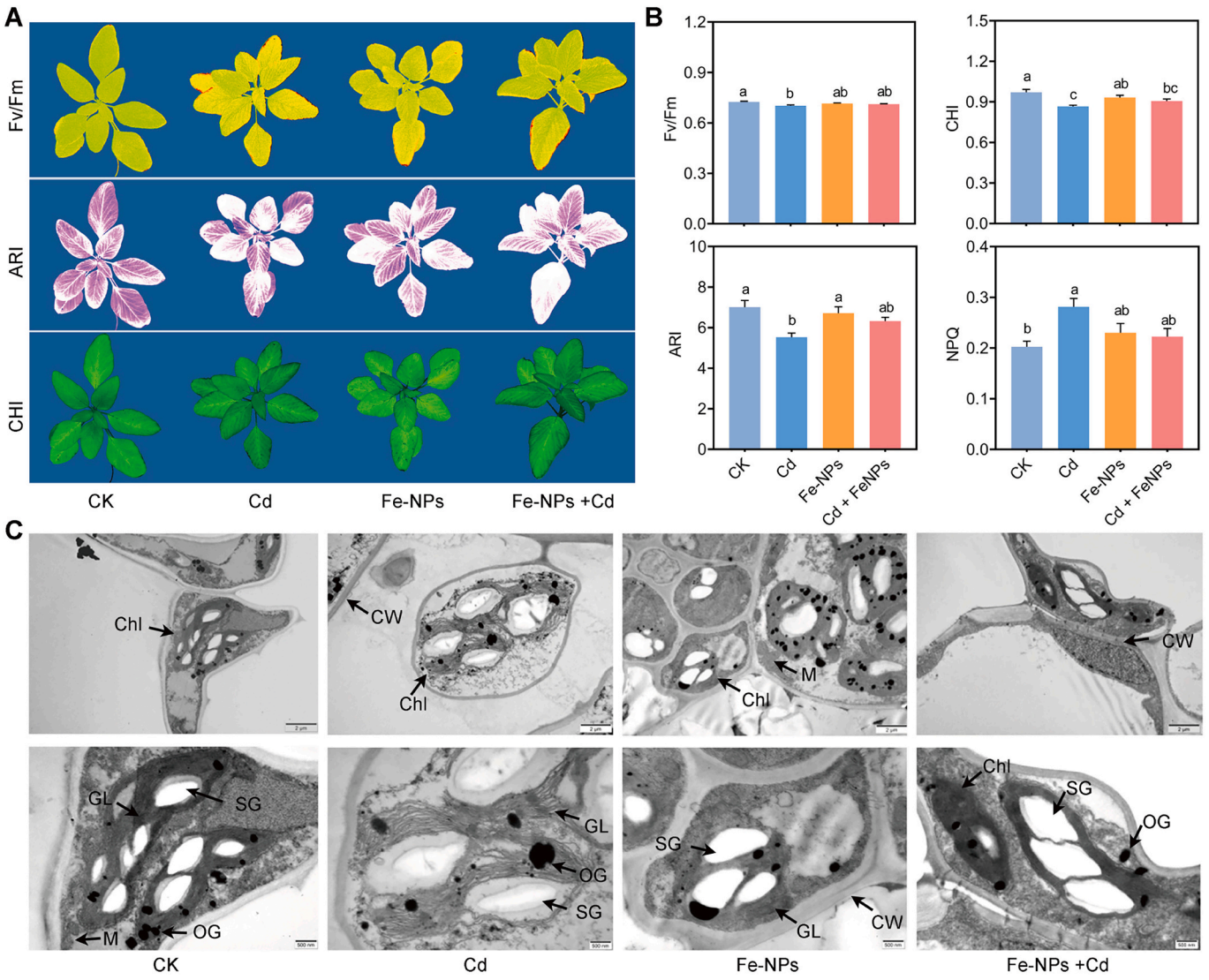

Fig. 2. The photosynthetic parameters and leaf ultrastructure characteristics of *A. hypochondriacus* under Cd, Fe-NPs, Fe-NPs + Cd, and control (CK, without Cd and Fe-NPs). (A) Representative fluocam false colour images of *A. hypochondriacus* leaves after 14 days treatments. (B) Quantitative analysis of leaf maximum quantum yield of PSII (F_v/F_m), Chlorophyll index (CHI), anthocyanin index (ARI) and non-photochemical quenching (NPQ). Values are means ± SE. Bar with different lowercase letters indicate significant differences between treatments according to one-way ANOVA and Turkey's tests ($p < 0.05$). (C) TEM images of leaf. Scale bar: 2 μm (upper) and 500 nm (down). Note: Cell wall, CW; Chlorophyll, Chl; mitochondria, M; Starch granules, SG; Grana lamellae, GL; Osmiophilic granule, OG.

genes exhibited similar expression patterns in *A. hypochondriacus* leaves after Fe-NPs and Cd treatments (Supplementary Fig. 7), confirming the reliability of the RNA-seq experiment.

GO enrichment analysis revealed that the DEGs of Cd_vs_CK were mainly enriched in DNA replication, protein folding and catalytic activity, plasma membrane, stress responses, ATP binding, and cell wall (Fig. 7B and Supplementary Table 4). Furthermore, more downregulated DEGs than upregulated DEGs were enriched in these GO terms, including the membrane, cytoplasm components, transport, protein catalytic activity, binding, and transcription factor activity (Supplementary Fig. 8 and Table 4). Additionally, DEGs associated with response to hydrogen peroxide, oxidoreductase activity, glutathione metabolic process, lignin biosynthetic process, and cell wall organization were downregulated under Cd stress (Supplementary Table 4). In contrast to the Cd group, DEGs in the Fe-NPs + Cd treatment were enriched in GO terms mainly related to the DNA-binding transcription factor activity, protein catalytic activity (phosphorylation, transferase, and endopeptidase), plant hormone-related processes, and responses to stress stimulus (Fig. 7B and Supplementary Table 4). Notably, a greater number of upregulated DEGs of Fe-NPs + Cd_vs_Cd comparison were significantly enriched in biological processes such as the regulation of DNA-templated transcription, hormone signaling, catalytic activity, and oxidation-reduction, and in cell component processes including the plasma membrane, nucleus, chloroplast, and cell wall, and in molecular function terms such as transcription factor activity, protein and DNA binding, and metal ions binding (Supplementary Fig. 8 and Supplementary Table 4). KEGG pathway analysis showed that Cd stress and Fe-NPs application significantly influenced the plant-pathogen interaction, MAPK signaling pathways, starch and sucrose metabolism, and secondary metabolic pathways (Fig. 7C and Supplementary Table 5). The most enriched pathways in Cd_vs_CK were associated with the DNA replication, MAPK signaling pathway, biotin metabolism, glutathione metabolism, ascorbate and aldarate metabolism, pentose and glucuronate metabolism. In the Fe-NPs + Cd_vs_Cd, more upregulated DEGs than downregulated DEGs were significantly enriched in pathways related to the plant-pathogen interaction, plant hormone signal transduction, glycerolipid metabolism, starch and sucrose metabolism (Supplementary Fig. 9 and Supplementary Table 5).

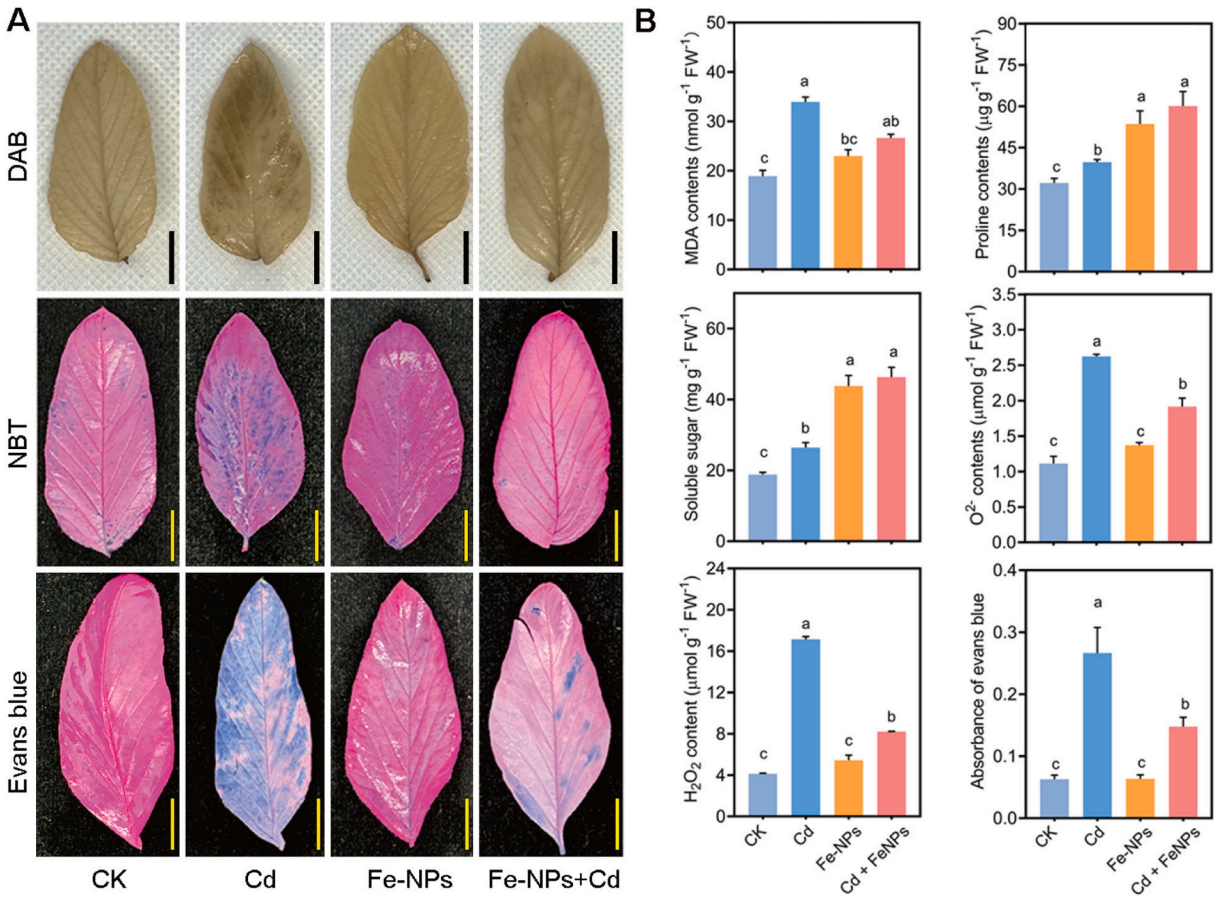

Fig. 3. Effects of Fe-NPs application on oxidative damage and ROS accumulation in leaves of *A. hypochondriacus* plants under Cd stress. (A) Visualization of H_2O_2 and O_2^- levels and cell viability in leaves stained with DAB, NBT, and evans blue, respectively. (B) The contents of malondialdehyde (MDA), proline, soluble sugar, $O_2^{\cdot-}$, H_2O_2, and the absorbance of evans blue. Values are means ± SE. Bar with different lowercase letters indicate significant differences between treatments according to one-way ANOVA and Turkey's tests ($p < 0.05$). (For interpretation of the references to colour in this figure legend, the reader is referred to the web version of this article.)

3.7. Effects of Fe-NPs on the key DEGs involved in ROS homeostasis, Cd transport, and cell wall modification

Given that significant enrichment for DEGs was observed in pathways related to oxidative stress regulation, metal ion transport, as well as cell wall synthesis (Supplementary Table 4), which are crucial processes impacting Cd tolerance [4], we proceeded to identify key genes in these categories and analyze their expression levels in the Cd_vs_CK and Fe-NPs + Cd_vs_Cd comparisons. Compared to CK, several metal transporters localized in the plasma membrane, such as detoxification efflux carriers (DTXs) (*AH011000*, *AH015007*, and *AH016653*), heavy metal-associated plant proteins (HIPPs) (*AH012098*, *AH018007*, and *AH022015*), and ZITs (*AH002109* and *AH017676*), as well as ABC transporter proteins (*AH015903*, *AH018912*, and *AH018045*) localized in the vacuole, were downregulated by Cd treatment (Fig. 8 and Supplementary Table 6). Conversely, these transcripts were significantly upregulated by Fe-NPs spraying under Cd stress (Fig. 8 and Supplementary Table 6). Interestingly, the expression levels of *NRAMP5* (*AH018497*), which is responsible for Cd influx, were higher in Cd_vs_CK than those in the Fe-NPs + Cd_vs_Cd comparison.

DEGs involved in antioxidant metabolism exhibited significant alterations in expression under Fe-NPs and Cd treatments (Fig. 8 and Supplementary Table 6). For instance, the overall expression of *peroxidase* (POD) was higher in the Fe-NPs + Cd_vs_Cd comparison than in Cd treatment alone. In contrast, DEGs encoding ascorbate oxidase (AP) and antioxidant protein thioredoxin (TRX), which are master regulators of the cellular redox balance, showed upregulation in Cd and Fe-NPs treatments. Additionally, several heat shock proteins (HSPs) exhibited different expression patterns in Cd_vs_CK and Fe-NPs + Cd_vs_Cd; four *HSPs* (*AH012734*, *AH010653*, *AH011911*, and *AH013669*) were significantly induced by Cd stress, while other *HSPs* were downregulated under Cd and Fe-NPs treatments. Furthermore, significant change was also found in the expression levels of genes related to glutathione metabolism between the Cd_vs_CK and Fe-NPs + Cd_vs_Cd. The glutamine synthetase (GLNT) gene (*AH001035*) and most *glutathione S-transferase* (*GST*) were upregulated in the Fe-NPs + Cd_vs_Cd compared to the Cd_vs_CK, while three identified *glutathione synthetase* (*GS, AH001035*, *AH019829*, and *AH015859*) involved in GSH synthesis were slightly induced by Fe-NPs + Cd or Cd alone (Fig. 8 and Supplementary Table 6).

Cell wall modification plays an important role in plant response to Cd stress [3]. Numerous DEGs related to the biosynthesis and signaling of the cell wall were identified in *A. hypochondriacus* leaves exposed to Fe-NPs and Cd treatments. These genes included PODs and laccases (LACs) involved in lignin synthesis, pectate lyase (PL), pectin methylesterase (PME), pectin methylesterase inhibitor (PMEI), polygalacturonase (PG), polygalacturonase inhibitor (PGIP), cellulose synthesis (CES), expansion protein (EXP), cell wall-associated receptor-like kinases (WAKLs), glycosyl transferases, and several glycosyl hydrolases (Fig. 8 and Supplementary Table 6). Most of these genes, such as *PODs*, *LAC*, *PGs, EXPs*, *CESs, PMEs/PMEI,* and *PLs* were upregulated in response to Cd stress, especially with the combined treatment of Fe-NPs and Cd. Notably, the reverse expression patterns of two *PG/PGIP* genes *(AH009734* and *AH020345),* three *XTH* genes (*AH008756*, *AH019221*, and *AH019219*)

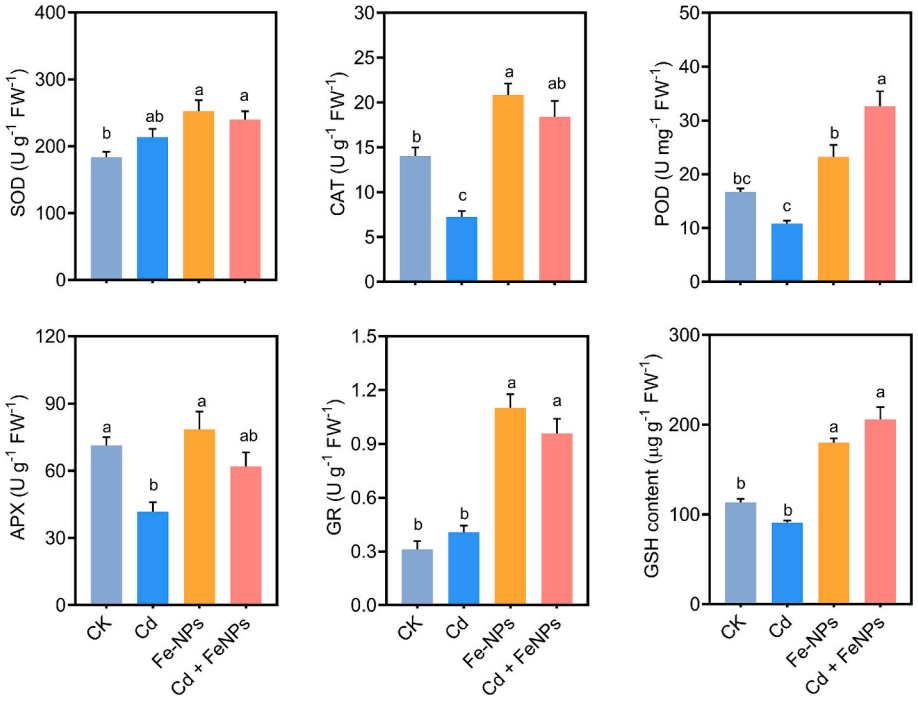

Fig. 4. Antioxidant enzyme activities and glutathione content in leaves of *A. hypochondriacus* treated with Fe-NPs and Cd. After 14 days of different treatments, the contents of glutathione (GSH) and the activities of superoxide dismutase (SOD), catalase (CAT), peroxidase (POD), ascorbate peroxidase (APX), and glutathione reductase (GR) were determined. The data are presented as the mean ± SE. Bars with different letters indicate significant differences among treatments ($p < 0.05$).

and six *PODs* were also observed between the Cd_vs_CK and Fe-NPs + Cd_vs_Cd comparisons. Also, many of carbohydrate-active genes coding xyloglucan endoglycosylase/hydrolase (XTHs), β-1,3-glucanase, glucan endo-1,3-beta-D-glucosidase, UDP-glycosyltransferase, invertase, and β-D-galactosidase which are required for cell wall loosening and elongation, formation of the secondary cell walls, were differentially regulated by Fe-NPs under Cd stress (Supplementary Table 3 and Table 6). Notably, genes encoding wall-associated receptor-like kinases (WAKLs) were all downregulated by Cd treatments. Members of this family, which have been reported to mediate cell wall signaling and Cd tolerance in plant [36,37]. However, this downregulation was mitigated by Fe-NPs application (Fig. 8 and Supplementary Table 6). These findings highlight the important role of cell wall metabolism and signaling in enhancing Cd tolerance with Fe-NPs.

3.8. Overexpression of AhWAKL16 increases Cd tolerance in A. hypochondriacus

The differential expression of the *AhWAKL* gene family observed in RNA-seq data encourages further investigation into the role of *AhWAKL* genes in Cd tolerance. Consequently, a member of the *AhWAKL* family, *AhWAKL16* (*AH011677*), which was significantly downregulated under Cd stress (Supplementary Table 6), was successfully cloned from *A. hypochondriacus* (Supplementary Fig. 10 A). Phylogenetic analysis showed that AhWAKL16 is clustered into a clade with those homologs from *Amaranthus tricolor*, *Beta Vulgaris*, and *Chenopodium quinoa* (Supplementary Fig. 10B), whereas its closest homolog WAK2 (*AT1G21270*) in *Arabidopsis*, clusters into a clade with homologs from *Glycine*, *Gossypium hirsutum*, and *Corymbia*. The tissue expression pattern of *AhWAKL16* in *A. hypochondriacus* revealed that it is most highly expressed in roots, stems, and flowers (Supplementary Fig. 10C). To validate its expression in response to Cd and Fe-NPs treatments, qRT-PCR analysis was performed in *A. hypochondriacus* roots and leaves after 12 h, 48 h and 14 days of treatment (Supplementary Fig. 11). Early induction of *AhWAKL16* was observed in roots at 12 h, whereas *AhWAKL16* transcript levels were downregulated in both roots and leaves at 48 h, and 14 d under Cd stress. Interestingly, application of Fe-NPs alone did not affect *AhWAKL16* expression in roots but caused a slight and delayed induction in leaves at 14 days post-spraying with Fe-NPs (Supplementary Fig. 11).

To further investigate the function of *AhWAKL16* in Cd tolerance, we generated *A. hypochondriacus* transgenic hairy roots overexpressing *AhWAKL16* using an overexpression vector (Fig. 9A). The transgenic hairy roots were validated via GFP reporter and qRT-PCR analysis. *AhWAKL16* expression levels in the transgenic hairy roots were at least three folds higher than those in the empty vector (EV) controls (Fig. 9B). Under Cd stress, *AhWAKL16-OE* plants exhibited increased Cd tolerance, with longer roots and higher leaf chlorophyll content than the EV controls (Fig. 9C–F). Additionally, *AhWAKL16-OE* hairy roots accumulated less MDA than the EV roots under Cd treatment (Fig. 9G). Cd content in hairy roots of *AhWAKL16-OE* remained unchanged (Fig. 9H). However, the subcellular distribution of Cd in cell wall fraction was increased about 8.03 % in *AhWAKL16-OE* hairy roots, while Cd in the organelle fraction was reduced by 4.7 % compared to the EV controls (Fig. 9I). We hypothesized that *AhWAKL16* alters cell wall composition to enhance Cd fixation. To test this, the content of pectin, cellulose, and hemicellulose was determined in the transgenic hairy roots. We found that pectin increased by 15.79 % in *AhWAKL16-OE* hairy roots compared to the EV controls, but this increase was not statistically significant (Supplementary Fig. 12). No significant differences were detected in other cell wall components (Supplementary Fig. 12). Collectively, these results suggested that *AhWAKL16* likely enhances Cd tolerance in *A. hypochondriacus* by partially promoting Cd retention in the cell wall.

4. Discussion

NPs can enter plant tissues via epidermal cells, cuticles, or stomata, thus regulating plant growth, development, and stress tolerance [22]. Generally, the impact of these NPs on plants is in a dose-dependent manner, and is closely associated with their core components, size, structure, and application methods [22]. Previous studies have reported that the optimal working concentrations of Fe-NPs for boosting

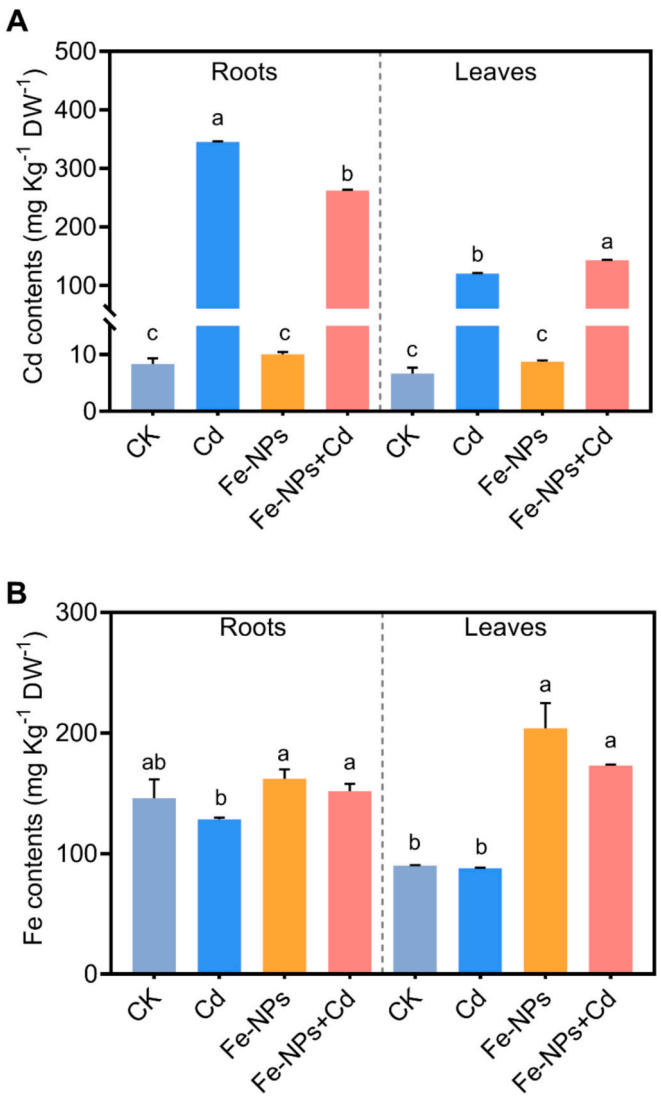

Fig. 5. Effects of Fe-NPs application on Cd content in *A. hypochondriacus* plants under Cd stress. (A) Cd concentrations in leaves and roots under Fe-NPs and Cd treatments for 14 days. (B) Fe concentrations in leaves and roots under Fe-NPs and Cd treatments. Values are means ± SE. Bars with different lowercase letters indicate significant differences among treatments according to one-way ANOVA and Turkey's tests ($p < 0.05$).

agricultural productivity can vary among different plant species. For example, seed treatment with Fe-NPs (Fe_3O_4) at 200 and 500 mg L^{-1} has been shown to improve wheat growth and leaf photosynthetic rate [26]. Zhang et al. [25] found that 10 mg L^{-1} of Fe-NPs ($FeCl_2$) is the effective concentration for promoting *Medicago* growth through seed-soaking and leaf-spraying. Another study analyzed the comparative effects of three forms Fe-NPs (α-Fe_2O_3, Y-Fe_2O_3, and Fe_3O_4) and two application methods (root irrigation versus leaf spraying) on growth parameters of maize. It revealed that root supplementation with 100 mg L^{-1} Fe-NPs (Fe_3O_4) can induce higher maize performance [32]. In soybean, foliar spraying of Fe-NPs (Fe_3O_4 or $Fe_7(PO_4)_6$) at 10 mg L^{-1} can improve soybean growth and nitrogen use efficiency, thereby increasing yield and quality [38]. Here, the effect of Fe-NPs (α-Fe_2O_3) on *A. hypochondriacus* growth and Cd tolerance was investigated through the foliar application. Among four different concentrations of Fe-NPs (50, 100, 200, and 500 mg L^{-1}), 100 mg L^{-1} was identified as the optimal and safe dose of Fe-NPs for enhancing Cd tolerance without inducing additional cell toxicity to *A. hypochondriacus* growth (Fig. 1, Supplementary Figs. 3 and 4). Understanding the absorption, transport, and accumulation dynamics of Fe-NPs is essential to evaluate their subsequent effects on plants. Surface charge of NPs is a critical factor influencing their rate of adherence to and penetration into leaf cells during foliar application [39]. Given that the plant cell walls and phospholipid membranes carry negative charges, positively charged Fe-NPs are known to exhibit preferential cuticle adherence and greater leaf accumulation compared to negatively charged Fe-NPs [37]. Although non-fluorescence labeled Fe-NPs used in this study prevented direct tracking, these nanoparticles showed a positive zeta potential (+ 4.66 mV, pH 7.0), and led to significantly higher Fe accumulation in both the leaves and roots of *A. hypochondriacus* treated with Fe-NPs alone, compared to the control plants (Fig. 5B). This indicates that Fe-NPs (α-Fe_2O_3) can be absorbed via leaf cuticles or stomata, subsequently altering the physiological characteristics of *A. hypochondriacus* under Cd stress.

Cd exposure for 14 days led to significant stress in *A. hypochondriacus*, as evidenced by reduced plant biomass (Fig. 1) and impaired photosynthetic capacity (Fig. 2). These findings are consistent with earlier reports about the physiological responses of *A. hypochondriacus* to Cd toxicity [18,19,21,40]. The decline in F_v/F_m indicated damage to PSII reaction centers, while the increase in NPQ suggested an enhanced energy dissipation mechanism to mitigate photodamage. Moreover, Cd stress resulted in a decline in CHI and ARI, indicating pigment degradation and impaired chloroplast function (Fig. 1). Previous studies verified that application of optimal concentrations of Fe-NPs to plant can enhance the photosynthesis via increasing the contents of chlorophyll [26,32,41], thereby promoting plant growth and stress tolerance including Cd toxicity [26,32,42,43]. Chlorophyll, as the primary pigment, plays a crucial role in plants by harvesting light energy and transforming it into chemical energy. The application of Fe-NPs in *A. hypochondriacus* also increased the chlorophyll content and partially elevated CHI and ARI values under Cd stress (Fig. 2A, B), suggesting that Fe-NPs alleviated Cd-induced pigment loss and contributed to maintaining chloroplast integrity. This mitigation effect was further supported by increasing the reduction in damage to the grana lamellae in chloroplasts (Fig. 2C), leading to enhanced photosynthetic performance, as reflected by the recovery of F_v/F_m. As an essential element, Fe participates in vital physiological and biochemical processes such as photosynthesis in chloroplasts and respiration in mitochondria [30]. It has been shown that Cd stress can induce Fe deficiency symptom [31], whereas exogenous Fe supplementation can alleviate the negative effects of Cd on photosynthesis in plants [44]. The present results indicated that foliar spraying of Fe-NPs significantly increased the Fe contents and chlorophyll production in leaves of *A. hypochondriacus* under Cd stress (Fig. 5B and Supplementary Fig. 5), suggesting that Fe-NPs may compensate for Cd-induced iron deficiency, a known driver of chlorophyll degradation [27,44]. Thus, it is not surprising that the application of Fe-NPs partially restores the structure and function of the entire photosynthetic apparatus in *A. hypochondriacus* plants treated with Cd.

Cd stress induces excessive ROS accumulation, leading to oxidative damage that accelerates pigment degradation and disrupts cellular metabolism [3]. One key mechanism underlying this protective effect of Fe-NPs in *A. hypochondriacus* appears to be the regulation of ROS homeostasis (Fig. 3 and Fig. 4). Earlier studies showed that certain Fe-NPs can maintain intracellular ROS homeostasis and improve plant resilience under abiotic stress through modulating the activity of antioxidant enzymes such as SOD, CAT, POD, APX, and GR [24,45]. The present study demonstrated that Fe-NPs alleviated oxidative damage by reducing MDA and ROS levels (Fig. 3), while increased the contents of proline and solute sugar, as well as the activities of antioxidant enzymes (POD, CAT, and GR) (Fig. 4). Similarly, application Fe_3O_4 nanoparticles to radish, decreasing ROS levels through improving APX, CAT, POD activities, which mitigated the adverse effects of cadmium [43]. Additionally, the transcriptomic analysis revealed that Fe-NPs upregulate antioxidant defense-related genes (*POD, GST, AP*, and *TRX*) in

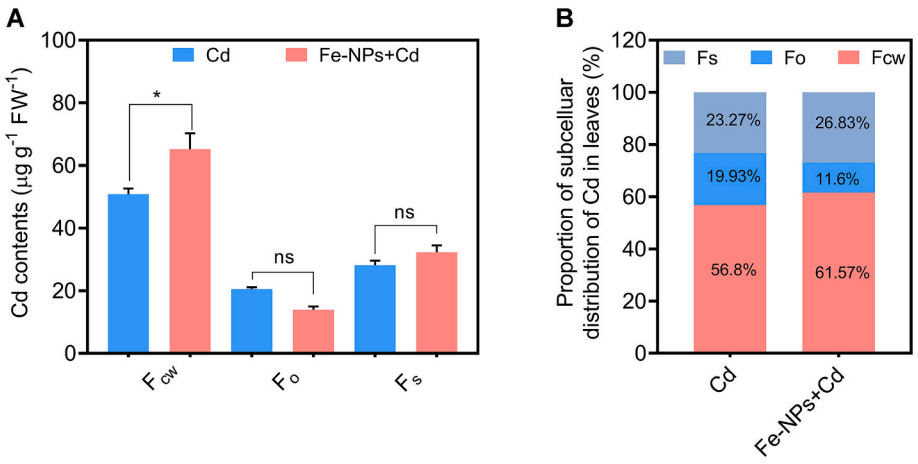

Fig. 6. Effects of Fe-NPs application on subcellular distribution of Cd in leaves of *A. hypochondriacus* plants under Cd stress. (A) Cd concentrations in cell wall fraction (F_w), organelles fraction (F_o), and soluble fraction (F_s) of leaves. (B) Proportion of Cd subcellular distribution in leaves. Error bars indicate the mean ± SE. Asterisk represents significant differences among treatments (*$p < 0.05$).

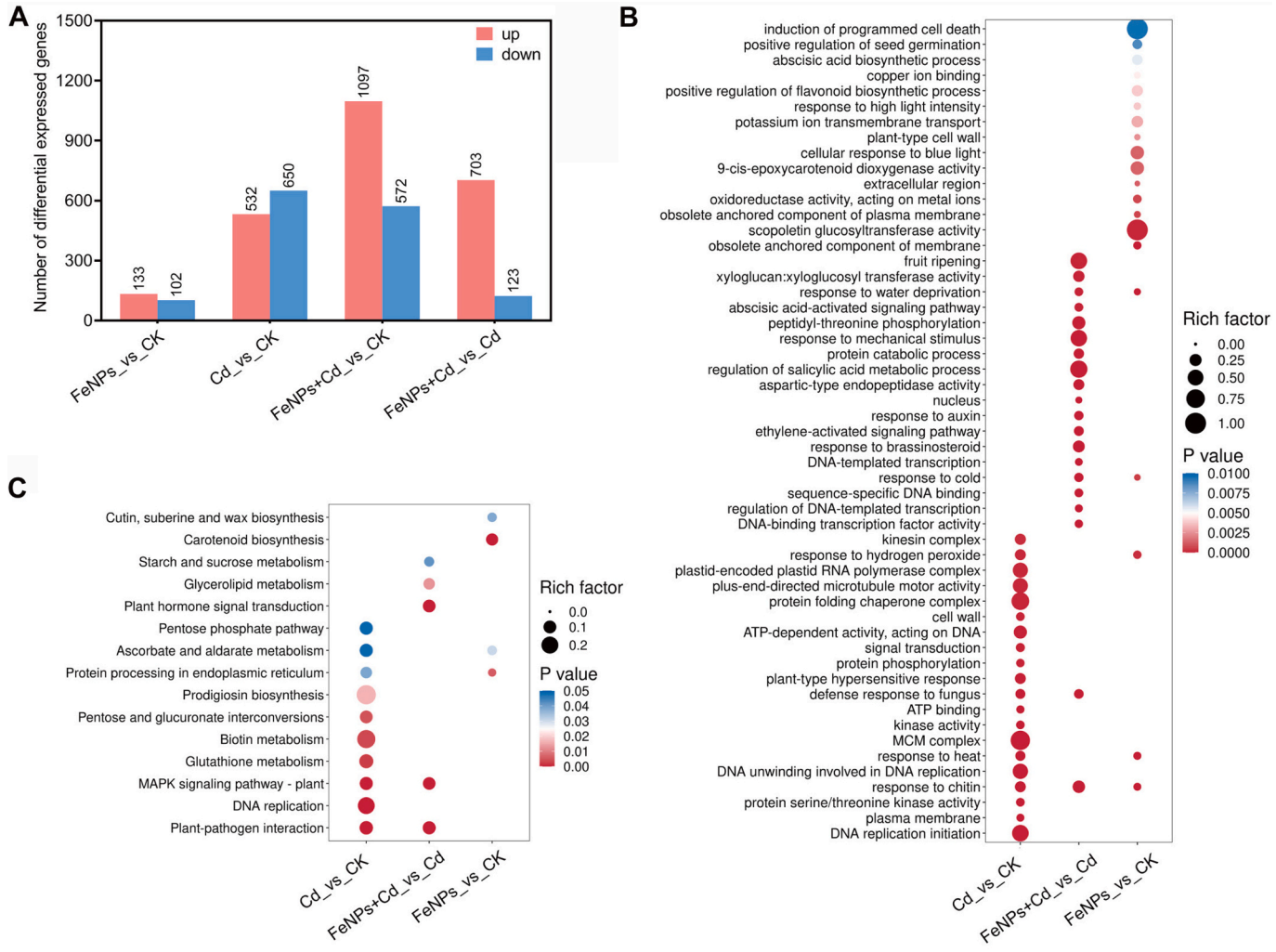

Fig. 7. Analysis of differentially expressed genes (DEGs) in leaves of *A. hypochondriacus* under Cd and Fe-NPs treatments for 14 days. (A) The number of DEGs in the comparisons of Cd vs CK, Fe-NPs_vs_CK, Fe-NPs + Cd_vs_CK, and Fe-NPs + Cd_vs_Cd. (B) GO analyasis of DEGs in the comparisons of Cd vs CK, Fe-NPs_vs_CK, and Fe-NPs + Cd_vs_Cd. (C) KEGG enrichment analysis of DEGs.

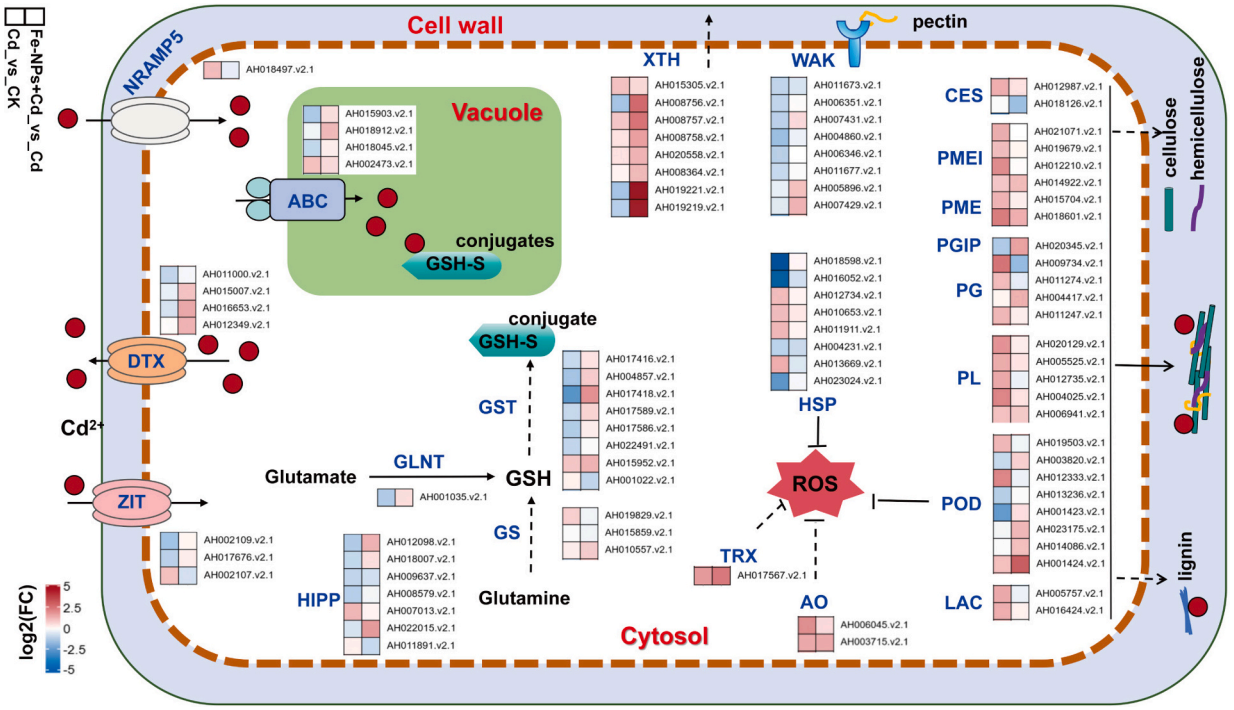

Fig. 8. Heatmap of the representative DEGs involved in Cd transport, cell wall biosynthesis, glutathione metabolism, and ROS metabolism under Cd and Fe-NPs treatments. The value is the $\log_2$fold change ($\log_2$(FC)) of each gene in the Cd vs CK, and Fe-NPs_vs_Cd comparisons. Red boxes represent upregulated genes and blue indicates downregulated genes. (For interpretation of the references to colour in this figure legend, the reader is referred to the web version of this article.)

A. hypochondriacus leaves under Cd stress (Fig. 8 and Supplementary Table 6), contributing to ROS scavenging and cellular protection. Together, these findings suggest that the alleviating effect of Fe-NPs on Cd toxicity in *A. hypochondriacus* leaves is closely associated with enhanced antioxidant capacities.

Plant biomass and the Cd concentration are key factors influencing Cd uptake, while low plant biomass is a major limitation for Cd phytoremediation efficiency [3]. As a hyperaccumulator of Cd, *A. hypochondriacus* exhibits relatively faster growth rates and higher biomass production than other plant species, which contribute to its potential for Cd phytoremediation [9,13,46]. In this study, Fe-NPs significantly increased leaf Cd contents but decreased root Cd contents in *A. hypochondriacus* plants compared to Cd treatment alone (Fig. 5A). Given that the majority of the biomass in *A. hypochondriacus* plants consists of aboveground tissues, it is reasonable to infer that the increased leaf biomass of *A. hypochondriacus* plants, induced by Fe-NPs under Cd stress, contributed to the enhanced Cd accumulation in leaves. Consistently, the increased Cd extraction amounts were observed in Fe-NPs-treated *A. hypochondriacus* plants compared to those treated with Cd alone (Supplementary Table 2), suggesting that foliar spraying of Fe-NPs promoted Cd phytoremediation in *A. hypochondriacus*. Similarly, researchers reported that appropriate plant hormones and microorganisms supply can also increase Cd accumulation in the aboveground tissues of *A. hypochondriacus* due to the enhancement of plant biomass [20,21]. Additionally, the optimal concentration of Fe-NPs has also been shown to increase biomass of *Medicago sativa* [25], rice [29], and maize [32] and heavy metal tolerance [23,24]. Thus, the current study provides additional evidence that the integration of exogenous Fe-NPs into agricultural practices can enhance Cd phytoextraction [23,43,47].

Regulation of subcellular Cd distribution is an important detoxification mechanism in plants, primarily through sequestration in the cell wall and vacuoles [4]. The plant cell wall, composed of cellulose, hemicellulose, pectin, and proteins, forms a special mesh-like structure that not only provides mechanical support but also acts as the first physical barrier against Cd entry by immobilization [4]. Once Cd fixation in the cell wall reaches saturation, excess Cd binds with chelating compounds to form nontoxic complexes, which are then transferred into vacuoles to reduce toxicity [4]. Previous reports have shown that applications of Zn or boron (B) increased Cd fixation in the cell wall of *Brassica napus* [48], rice [49], hot pepper [50], and water spinach [51], restricting its entry into the cytoplasm and reducing Cd toxicity. Similarly, Cd compartmentalization in the cell wall is also associated with enhanced Cd tolerance in *A. hypochondriacus* induced by Se [34] and rutin [18]. Consistent with the above reports, Fe-NPs increased the proportion of Cd in the cell wall fraction of leaves from 57 % to 62 % and in the solution fraction (including vacuoles) from 23 % to 27 %, while reducing the proportion of Cd in the organelle fraction by about 8.33 % under Cd treatment (Fig. 6). These results indicate that application of Fe-NPs promotes Cd immobilization and compartmentalization in the cell wall and vacuoles of *A. hypochondriacus* leaves, thereby reducing Cd toxicity. Excessive Cd accumulation in organelles can disrupt the structure and function of chloroplasts and mitochondria [3,4]. Thus, the immobilization of Cd in the cell wall and vacuoles induced by Fe-NPs may decrease Cd accumulation in organelles, aiding the restoration of chloroplasts and mitochondria functions. Taken together, these findings imply that Fe-NPs-induced Cd retention in the cell walls and vacuoles may contribute to Cd tolerance in *A. hypochondriacus* leaves.

Cd uptake and translocation in plants are mediated by specific ion transporter proteins located on the membrane, such as natural resistance-associated macrophage proteins (NRAMP), iron-regulated transporter proteins (ZIT), metal tolerance proteins (MTP), and heavy-metal-transporting ATPase (HMA) family members [3,4]. Transcriptome analysis revealed that Fe-NPs differentially regulated a series of *A. hypochondriacus* genes related to Cd absorption and transport (*NRAMP*, *ZIPs*, *DTXs*, *ABCs*, and *HIPPs*) under Cd stress (Fig. 7, Fig. 8 and Supplementary Table 6), which may contribute to the increased Cd concentration in Fe-NP-treated leaves. Previous research indicated that *NRAMP1* and *NRAMP5* are involved in the uptake and transport of Cd, Fe, and Mn [52,53]. Knockout of *OsNRAMP5* enhanced Cd translocation

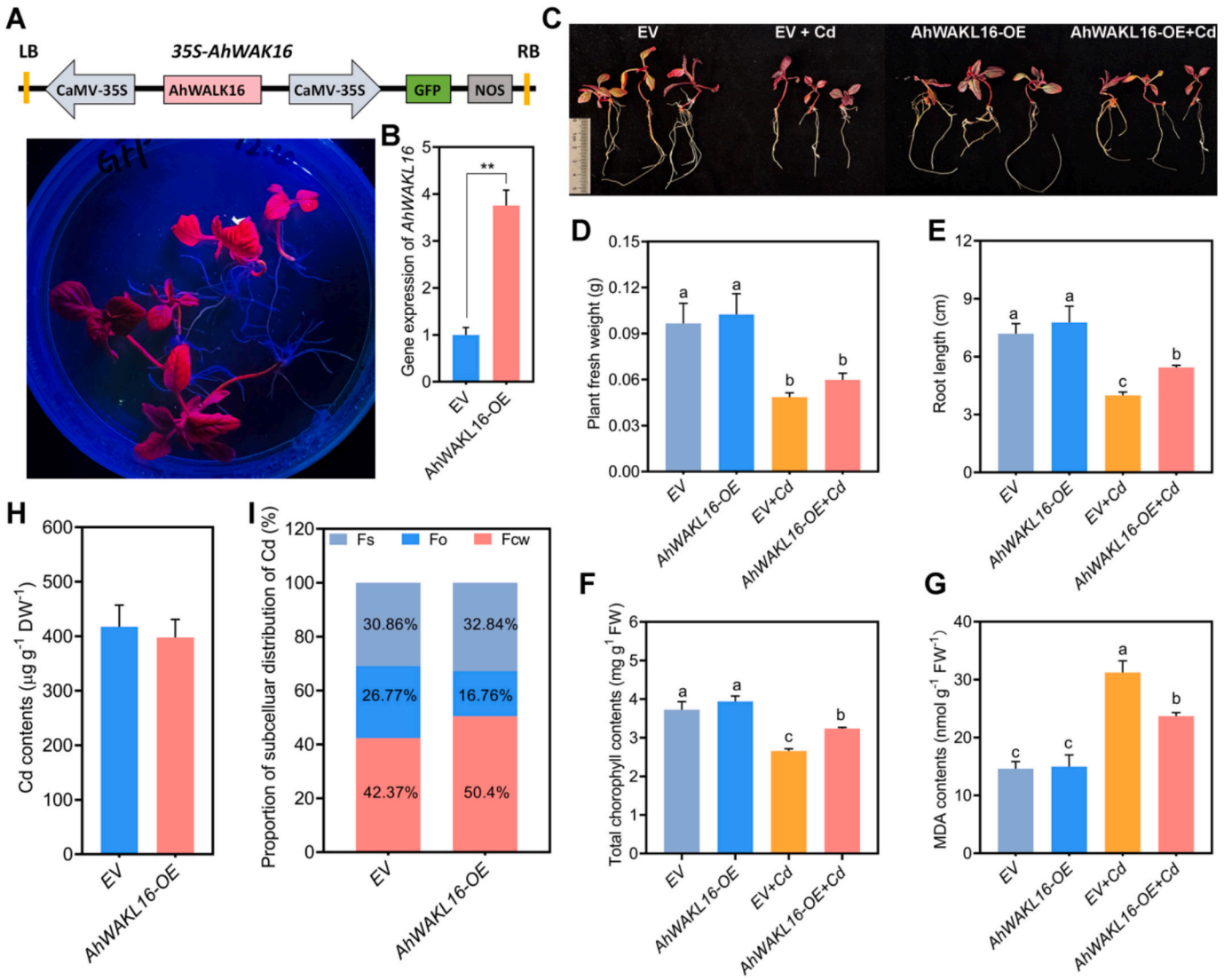

Fig. 9. Study of the role of *AhWAKL16* in Cd tolerance using *A. hypochondriacus* transgenic hairy roots. (A) Diagram of the *AhWAKL16* overexpressing vector harboring the *GFP* marker. (B) Validation of the relative *AhWAKL16* expression levels in transgenic hairy roots of *A. hypochondriacus* using qRT-PCR. Error bars indicate the means ± SE, $^{**}p < 0.01$. (C) The growth phenotype of the *AhWAKL16-OE* and *EV* composite plants grown in 1/2 MS plates containing 50 μmol L^{-1} $CdCl_2$ for 7 days. (D) Plant fresh biomass. (E) Hairy root length. (F) Total chlorophyll content of leaves. (G) MDA content of hairy roots. (H) Cd concentrations in *AhWAKL16-OE* and *EV* hairy roots under Cd stress. (I) Subcellular distribution of Cd in hairy roots of the *AhWAKL16-OE* and *EV* composite plants. Fw, cell wall fraction; Fo, organelles fraction; and Fs, soluble fraction. Error bars indicate the mean ± SE. Different lowercase letters represent significant differences among treatments ($p < 0.05$).

from roots to the shoots in rice, thereby increasing the efficient phytoremediation of Cd from paddy fields [54]. Here, *NRAMP5* in *A. hypochondriacus* was significantly upregulated by Cd, while Fe-NPs downregulated its expression under Cd stress (Fig. 8). This is consistent with the increased Fe content in *A. hypochondriacus* leaves by application of Fe-NPs (Fig. 5), suggesting that excessive Fe uptake in the leaves of *A. hypochondriacus* may cause a feedback inhibition in *NRAMP5* expression, thereby reducing Cd transmission. As important Zn/Cd transporters, ZITs affect Cd mobility in the xylem and transport to the above-ground parts [55]. The *DTX* gene family regulates Cd efflux from the cytoplasm [56], while HIPP proteins, belonging to metallothionein, play a role in Cd detoxification through binding and transport [57,58]. In rice, foliar application of Zn or melatonin altered the expression of ion transport-related genes (*NRAMPs*, *ZIPs*, *DTXs*, *HIPPs)* to reduce Cd toxicity [49,59]. In sweet potato, potassium (K) supply reportedly increased Cd retention in the root vacuoles and reduced Cd translocation to the shoot by inhibiting the expression of iron-regulated transporter (*IRT1*), copper transporter 5 (*COPT5*), and *NRAMP3* [60]. In hot peppers, B application also improved Cd sequestration and tolerance by increasing the expression levels of genes related to *HIPP*, vacuolar cation/proton exchanger (*CAX3*), *ABP*, *ZIP*, and *DTX* [50]. Consistently, Fe-NPs substantially increased the expression of *ZIPs*, *HIPPs*, and *DTXs* in Cd-treated *A. hypochondriacus* plants compared to the Cd treatment alone. Additionally, several ABC transporters, responsible for vacuoles Cd sequestration [61,62], were downregulated by Cd treatment but upregulated by Fe-NPs under Cd stress. This suggests that Fe-NPs-induced upregulation of ABC transporters could contribute to Cd compartmentalization in vacuoles. Previous findings showed that GSH and phytochelatin synthesis play crucial roles in Cd detoxification and tolerance by forming Cd-GSH and Cd-phytochelatin complexes, facilitating Cd translocation and vacuole sequestration [63,64]. Elevated GSH and phytochelatin levels and activities of enzymes involved in GSH synthesis promote Cd accumulation and enhance Cd tolerance in plants [4,65]. Similarly, Fe-NPs activated the expression of key GSH biosynthesis genes including *GLNT*, *GS*, and *GST* under Cd stress (Fig. 8 and Supplementary Table 6), and GSH levels in *A. hypochondriacus* leaves

were significantly elevated by Fe-NPs alone or in combination with Cd (Fig. 4), suggesting that Fe-NPs might enhance Cd chelation and fixation by regulating GSH synthesis.

GO cellular component analysis indicated that many DEGs were significantly enriched in the cell wall process under Cd and Fe-NPs treatments (Fig. 7B and Supplementary Table 4). This further supports the conclusion that transcriptional regulation of the cell wall to limit Cd mobility is a conserved mechanism of hyperaccumulators against Cd stress [4]. Plant cell wall modification is facilitated by a set of enzymes and proteins, including PME, PMEI, EXP, PG, PGIP, CES, LAC, glycosyl transferases, and glycosyl hydrolases [66]. Importantly, Fe-NPs significantly impacted the expression of genes involved in pectin and cellulose metabolism (Fig. 8 and Supplementary Table 6). Pectin and hemicellulose play crucial roles in retaining Cd in the plant cell wall, and their contents are positively related to Cd tolerance [48,67]. Pectin demethylation by PME releases more carboxyl groups that bind Cd [68,69], whereas PMEI negatively regulates this process [48]. Furthermore, the downregulation of *pectin lyase* (*PL*) genes increases in pectin content and enhances Cd tolerance by reducing pectin degradation [48]. In this study, *PME* genes were significantly upregulated by Cd and Fe-NPs treatments. However, the expression levels of major *PMEI* and *PL* genes were obviously lower in the Fe-NPs + Cd group than in the Cd treatment alone. This suggests that Fe-NPs may promote higher levels of demethylated pectin in *A. hypochondriacus* leaves under Cd stress by modulating pectin-modifying genes, thereby enhancing Cd accumulation in the cell wall. Lignin also contributes to Cd fixation in the cell wall [70,71]. The elevated lignin synthesis through enzymes such as phenylalanine ammonia-lyase (PAL), caffeic acid *O*-methyltransferase (COMT), and POD reduces Cd toxicity [70,71]. Supporting this, we observed more upregulated *POD* genes in leaves of the Fe-NPs + Cd group than in the Cd-treated plants. This suggests that Fe-NPs may stimulate lignin biosynthesis and Cd binding with lignin. Additionally, obvious changes were observed in the transcriptional levels of several other cell wall-related genes induced by Fe-NPs under Cd stress, including *PG, PGIP, CES, EXP, XTHs,* and *UDP-glycosyltransferase*, which are involved in cell wall formation and modification [59]. Collectively, these gene expression changes indicate that Fe-NPs positively influence Cd adsorption in *A. hypochondriacus* leaf cell walls through transcriptional remodeling. Nevertheless, further research should examine how Fe-NPs influence specific cell wall components (cellulose, hemicellulose, pectin, and lignin) and Cd distribution among them in *A. hypochondriacus* under Cd stress. Such investigations will clarify their precise roles in Fe-NPs-mediated Cd tolerance and provide more definitive evidence supporting the transcriptomic observations.

WAKs/WAKLs belong to the receptor-like protein kinases (RLKs) family and can sense and/or transduce the cell wall signals through binding to pectin [72]. Increasing evidence has shown that WAKs/WAKLs mediate plant responses to heavy metal stresses. Examples included *WAK11* in rice [73], *WAK1* [74], *WAKL4* [37,75] and *WAKL11* [36] in *Arabidopsis*, and *VuWAK1* in *Vigna umbellata* [76], all of which are transcriptionally responsive to heavy metals such as Al, Zn, Fe, Cu, Mn, and Cd. Moreover, overexpression of *WAK1* in *Arabidopsis* enhances Al tolerance [74], while knockdown of *WAKL4* increases *Arabidopsis* sensitivity to Cu or Zn [75]. We here showed that the *AhWAKL* gene family exhibited downregulation in response to Cd stress (Fig. 8). However, their expression levels were upregulated by Fe-NPs in *A. hypochondriacus* leaves under Cd stress, suggesting the potential role of *AhWAKLs* in *A. hypochondriacus* coping with Cd stress. We then focused on a representative *AhWAKLs* member, *AhWAKL16* (Supplementary Fig. 10), and confirmed its role in modulating Cd tolerance based on the following experimental evidence. First, *AhWAKL16* expression is Cd-responsive in roots and leaves of *A. hypochondriacus* (Supplementary Fig. 11). Second, *AhWAKL16*-overexpressing hairy roots exhibited enhanced Cd tolerance (Fig. 9). Third, *AhWAKL16* overexpression increases both pectin content and the distribution ratio of Cd in the cell wall (Fig. 9 and Supplementary Fig. 12). These observations suggest that *AhWAKL16* may regulate Cd tolerance in *A. hypochondriacus* through partially increaing pectin content and promoting Cd retention in the cell wall. Previous studies indicated that modulation pectin content and demethylation can immobilize Cd in plant cell walls [48,77]. For example, B application promotes pectin synthesis and demethylation, increasing Cd binding to ionic soluble pectin in *Brassica napus* shoots and thereby enhancing cell wall Cd retention and tolerance [77]. However, the correlation between WAK-mediated pectin metabolism and Cd tolerance appears complex. Contrasting with our *AhWAKL16* results, *Arabidopsis* overexpressing *WAK11* reduced pectin content and Cd accumulation in cell wall compared to WT, thereby decreasing Cd sensitivity [36]. These differences may be due to the distinct physiological functions of *WAKs/WAKLs* across different plant species or tissues. Furthermore, a very recent study showed that WAKL4-mediated phosphorylation of the Cd transporter NRAMP1 enhances vacuole-targeted ubiquitination and degradation, consequently limiting Cd absorption in *Arabidopsis* roots [37]. As AhWAKL16 potentially acts as a protein kinase, its role in cell wall Cd retention may rely on phosphorylation of key potential targets (e.g., Cd transporters or cell wall proteins). Thus, the precise mechanism requires further investigation.

Despite the multifaceted benefits of Fe-NPs in promoting crop production, enhancing plant resistance, and soil pollution remediation [23–29], their potential environmental risks to natural ecosystems cannot be overlooked. For example, prolonged agricultural exposure to Fe-NPs can induce oxidative stress in living organisms [78]. Moreover, the increasing Fe-NPs applications may facilitate soil leaching (e.g., via rainfall or human activities), adversely impacting soil microorganisms and disrupting critical microbial metabolic reactions such as the rhizosphere Fenton reaction [79]. Foliar application of Fe-NPs in agriculture also risks excess Fe accumulation in underground tissues, potentially causing Fe toxicity in plants. In this context, long-term investigation should be conducted to assess the ecotoxicity of Fe-NPs while utilizing their positive effects on Cd remediation in future research. Overall, establishing standardized protocols for the safe implementation of Fe-NPs technologies in Cd remediation is urgently required.

5. Conclusion

This work demonstrated that Fe-NPs application enhances Cd tolerance in *A. hypochondriacus* by boosting photosynthetic capacity and maintaining cellular redox homeostasis, thereby mitigating Cd-induced growth inhibition. Foliar spraying of Fe-NPs altered Cd transport and promoted Cd immobilization in leaf cell wall through transcriptional regulation of key genes involved in cell wall metabolism and ion transport. Additionally, *AhWAKL16* was identified as a positive regulator of Cd tolerance, potentially linked to increased pectin levels and enhanced cell wall Cd retention. Collectively, these findings provide valuable insights into the molecular mechanisms underlying Fe-NPs-induced Cd tolerance in *A. hypochondriacus* and broaden the potential applications of Fe-NPs in Cd phytoremediation strategies. To our knowledge, this is the first report linking Fe-NPs to *WAKL*-mediated cell wall Cd immobilization in a hyperaccumulator, providing a novel molecular target for Cd phytoremediation.

CRediT authorship contribution statement

Yanfeng Hu: Writing – original draft, Validation, Methodology, Investigation, Formal analysis, Data curation, Conceptualization. **Jia You:** Writing – original draft, Validation, Investigation, Formal analysis. **Yue Xiang:** Resources, Investigation. **Runze Tian:** Resources, Investigation. **Jianli Wang:** Resources, Investigation. **Zhongbao Shen:** Validation, Funding acquisition. **Yansheng Li:** Writing – review & editing, Validation, Funding acquisition, Conceptualization.

Declaration of competing interest

The authors declare that they have no conflict of interest.

Acknowledgments

This work was supported by Funds for the Strategic Priority Research Program of the Chinese Academy of Sciences (XDA28100200), the Youth Innovation Promotion Association of CAS (2020236) and Leap Engineering Major Needs Science and Technology Innovation Key Program in Heilongjiang Province (CX23ZD04).

Appendix A. Supplementary data

Supplementary data to this article can be found online at https://doi.org/10.1016/j.enceco.2025.06.015.

Data availability

Data will be made available on request.

References

[1] S. Kumar, A. Sharma, Cadmium toxicity: effects on human reproduction and fertility, Rev. Environ. Health 34 (2019) 327–338, https://doi.org/10.1515/reveh-2019-0016.
[2] Y. Huang, C. He, C. Shen, J. Guo, S. Mubeen, J. Yuan, Z. Yang, Toxicity of cadmium and its health risks from leafy vegetable consumption, Food Funct. 8 (2017) 1373–1401, https://doi.org/10.1039/c6fo01580h.
[3] N. Shaari, M. Tajudin, M. Khandaker, A. Majrashi, M. Alenazi, U. Abdullahi, K. Mohd, Cadmium toxicity symptoms and uptake mechanism in plants: a review, Braz. J. Biol. 84 (2022) e252143.
[4] J.S. Luo, Z. Zhang, Mechanisms of cadmium phytoremediation and detoxification in plants, Crop J. 9 (2021) 521–529, https://doi.org/10.1016/j.cj.2021.02.001.
[5] N. Verbruggen, M. Juraniec, C. Baliardini, C.L. Meyer, Tolerance to cadmium in plants: the special case of hyperaccumulators, Biometals 26 (2013) 633–638, https://doi.org/10.1007/s10534-013-9659-6.
[6] R. Huang, M. Dong, P. Mao, P. Zhuang, J. Paz-Ferreiro, Y. Li, Y. Li, X. Hu, P. Netherway, Z. Li, Evaluation of phytoremediation potential of five Cd (hyper) accumulators in two Cd contaminated soils, Sci. Total Environ. 721 (2020) 137581, https://doi.org/10.1016/j.scitotenv.2020.137581.
[7] X. Zhang, H. Xia, Z. Li, P. Zhuang, B. Gao, Identification of a new potential Cd-hyperaccumulator Solanum photeinocarpum by soil seed bank-metal concentration gradient method, J. Hazard. Mater. 189 (2011) 414–419, https://doi.org/10.1016/j.jhazmat.2011.02.053.
[8] E.G. Tovar-Perez, A. Lugo-Radillo, S. Aguilera-Aguirre, Amaranth grain as a potential source of biologically active peptides: a review of their identification, production, bioactivity, and characterization, Food Rev. Int. 35 (2019) 221–245, https://doi.org/10.1080/87559129.2018.1514625.
[9] N.Y. Li, Q.L. Fu, P. Zhuang, B. Guo, B. Zou, Z.A. Li, Effect of fertilizers on Cd uptake of *Amaranthus hypochondriacus*, a high biomass, fast growing and easily cultivated potential Cd hyperaccumulator, Int. J. Phytoremediat. 14 (2012) 162–173, https://doi.org/10.1080/15226514.2011.587479.
[10] A.J.M. Baker, R.R. Brooks, Terrestrial higher plants which hyperaccumulate metallic elements—a review of their distribution, ecology and phytochemistry, Biorecovery 1 (1989) 81–126.
[11] X. Zhang, S. Zhang, X. Xu, T. Li, G. Gong, Y. Jia, Y. Li, L. Deng, Tolerance and accumulation characteristics of cadmium in *Amaranthus hybridus* L, J. Hazard. Mater. 180 (2010) 303–308, https://doi.org/10.1016/j.jhazmat.2010.04.031.
[12] S. Liu, S. Ali, R. Yang, J. Tao, B. Ren, A newly discovered Cd-hyperaccumulator *Lantana camara* L, J. Hazard. Mater. 371 (2019) 233–242, https://doi.org/10.1016/j.jhazmat.2019.03.016.
[13] J. Guo, G. Zheng, J. Yang, T. Chen, X. Meng, T. Xia, Safe utilization of cadmium- and lead-contaminated farmland by cultivating a winter rapeseed/maize rotation compared with two phytoextraction approaches, J. Environ. Manag. 304 (2022) 114306, https://doi.org/10.1016/j.jenvman.2021.114306.
[14] D. Guo, A. Ali, C. Ren, J. Du, R. Li, A.H. Lahori, R. Xiao, Z. Zhang, Z. Zhang, EDTA and organic acids assisted phytoextraction of Cd and Zn from a smelter contaminated soil by potherb mustard (*Brassica juncea, Coss*) and evaluation of its bioindicators, Ecotoxicol. Environ. Saf. 167 (2019) 396–403, https://doi.org/10.1016/j.ecoenv.2018.10.038.
[15] Y. Hu, X. Zhou, A. Shi, Y. Yu, C. Rensing, T. Zhang, S. Xing, W. Yang, Exogenous silicon promotes cadmium (Cd) accumulation in *Sedum alfredii* Hance by enhancing Cd uptake and alleviating Cd toxicity, Front. Plant Sci. 14 (2023) 1134370, https://doi.org/10.3389/fpls.2023.1134370.
[16] Z. Chen, Q. Liu, S. Zhang, Y. Hamid, J. Lian, X. Huang, T. Zou, Q. Lin, Y. Feng, Z. He, X. Yang, Foliar application of plant growth regulators for enhancing heavy metal phytoextraction efficiency by *Sedum alfredii* Hance in contaminated soils: lab to field experiments, Sci. Total Environ. 913 (2024) 169788, https://doi.org/10.1016/j.scitotenv.2023.169788.
[17] B. Wu, T. He, Z. Wang, S. Qiao, Y. Wang, F. Xu, H. Xu, Insight into the mechanisms of plant growth promoting strain *SNB6* on enhancing the phytoextraction in cadmium contaminated soil, J. Hazard. Mater. 385 (2020) 121587, https://doi.org/10.1016/j.jhazmat.2019.121587.
[18] Y. Kang, J. Liu, L. Yang, N. Li, Y. Wang, T. Ao, W. Chen, Foliar application of flavonoids (rutin) regulates phytoremediation efficiency of *Amaranthus hypochondriacus* L. by altering the permeability of cell membranes and immobilizing excess Cd in the cell wall, J. Hazard. Mater. 425 (2022) 127875, https://doi.org/10.1016/j.jhazmat.2021.127875.
[19] N. Li, J. Liu, L. Yang, Y. Kang, Y. Cao, K. Chen, H. Sun, W. Chen, Q. Dai, Y. Sakai, Synergistic effect of antioxidant systems enhance cadmium phytoextraction and translocation in *Amaranthus hypochondriacus* under rutin application, S. Afr. J. Bot. 149 (2022) 582–590, https://doi.org/10.1016/j.sajb.2022.06.053.
[20] S. Sun, X. Zhou, X. Cui, C. Liu, Y. Fan, M.B. McBride, Y. Li, Z. Li, P. Zhuang, Exogenous plant growth regulators improved phytoextraction efficiency by *Amaranths hypochondriacus* L. in cadmium contaminated soil, Plant Growth Regul. 90 (2020) 29–40, https://doi.org/10.1007/s10725-019-00548-5.
[21] S. Cao, W. Wang, F. Wang, J. Zhang, Z. Wang, S. Yang, Q. Xue, Drought-tolerant *Streptomyces pactum* Act12 assist phytoremediation of cadmium-contaminated soil by *Amaranthus hypochondriacus*: great potential application in arid/semi-arid areas, Environ. Sci. Pollut. Res. 23 (2016) 14898–14907, https://doi.org/10.1007/s11356-016-6636-y.
[22] J. Wang, H. Wu, Y. Wang, W. Ye, X. Kong, Z. Yin, Small particles, big effects: how nanoparticles can enhance plant growth in favorable and harsh conditions, J. Integr. Plant Biol. 66 (2024) 1274–1294, https://doi.org/10.1111/jipb.13652.
[23] J. Lin, F. He, B. Su, M. Sun, G. Owens, Z. Chen, The stabilizing mechanism of cadmium in contaminated soil using green synthesized iron oxide nanoparticles under long-term incubation, J. Hazard. Mater. 379 (2019) 120832, https://doi.org/10.1016/j.jhazmat.2019.120832.
[24] N. Manzoor, L. Ali, A.A. Al-Huqail, S.M.S. Alghanem, H.A.S. Al-Haithloul, T. Abbas, G. Chen, L. Huan, Y. Liu, G. Wang, Comparative efficacy of silicon and iron oxide nanoparticles towards improving the plant growth and mitigating arsenic toxicity in wheat (*Triticum aestivum* L.), Ecotoxicol. Environ. Saf. 264 (2023) 115382, https://doi.org/10.1016/j.ecoenv.2023.115382.
[25] M.X. Zhang, L.Y. Zhao, Y.Y. He, J.P. Hu, G.W. Hu, Y. Zhu, A. Khan, Y.C. Xiong, J. L. Zhang, Potential roles of iron nanomaterials in enhancing growth and nitrogen fixation and modulating rhizomicrobiome in alfalfa (*Medicago sativa* L.), Bioresour. Technol. 391 (2024) 129987, https://doi.org/10.1016/j.biortech.2023.129987.
[26] V.D.D. Kreslavski, A.N.N. Shmarev, A.A.A. Ivanov, S.K.K. Zharmukhamedov, V. Strokina, A. Kosobryukhov, M. Yu, S.I.I. Allakhverdiev, S. Shabala, Effects of iron oxide nanoparticles (Fe_3O_4) and salinity on growth, photosynthesis, antioxidant activity and distribution of mineral elements in wheat (*Triticum aestivum*), Funct. Plant Biol. 50 (2023) 932–940, https://doi.org/10.1071/fp23085.
[27] N. Manzoor, T. Ahmed, M. Noman, M. Shahid, M.M. Nazir, L. Ali, T.S. Alnusaire, B. Li, R. Schulin, G. Wang, Iron oxide nanoparticles ameliorated the cadmium and salinity stresses in wheat plants, facilitating photosynthetic pigments and restricting cadmium uptake, Sci. Total Environ. 769 (2021) 145221, https://doi.org/10.1016/j.scitotenv.2021.145221.
[28] C. Deng, Y. Wang, C. Castillo, Y. Zhao, W. Xu, J. Lian, K. Rodriguez-Otero, H. J. Brown, K. Cota-Ruiz, W.H. Elmer, C.O. Dimkpa, J.P. Giraldo, Y. Wang, R. Hernandez, J.C. White, Nanoscale iron (Fe_3O_4) surface charge controls fusarium suppression and nutrient accumulation in tomato (*Solanum lycopersicum* L.), ACS Sustain. Chem. Eng. 12 (2024) 13285–13296, https://doi.org/10.1021/acssuschemeng.4c04800.
[29] Y. Yu, Y. Feng, Y. Yu, L. Xue, L. Yang, L. Zhong, M. Delgado-Baquerizo, S. He, Closing the gap between climate regulation and food security with nano iron oxides, Nat. Sustain. 7 (2024) 758–765, https://doi.org/10.1038/s41893-024-01334-6.
[30] G. Vigani, G. Zocchi, K. Bashir, K. Philippar, J.F. Briat, Signals from chloroplasts and mitochondria for iron homeostasis regulation, Trends Plant Sci. 18 (2013) 305–311, https://doi.org/10.1016/j.tplants.2013.01.006.
[31] H. Bashir, M.I. Qureshi, M.M. Ibrahim, M. Iqbal, Chloroplast and photosystems: impact of cadmium and iron deficiency, Photosynthetica 53 (2015) 321–335, https://doi.org/10.1007/s11099-015-0152-z.
[32] N. Yousaf, M. Ishfaq, H.A. Qureshi, A. Saleem, H. Yang, M.F. Sardar, C. Zou, Characterization of root and foliar-applied iron oxide nanoparticles (α-Fe_2O_3, γ-Fe_2O_3, Fe_3O_4, and bulk Fe_3O_4) in improving maize (*Zea mays* L.) performance, Nanomaterials 13 (2023) 3036, https://doi.org/10.3390/nano13233036.
[33] M. Li, P. Zhang, M. Adeel, Z. Guo, A.J. Chetwynd, C. Ma, T. Bai, Y. Hao, Y. Rui, Physiological impacts of zero valent iron, Fe_3O_4 and Fe_2O_3 nanoparticles in rice plants and their potential as Fe fertilizers, Environ. Pollut. 269 (2020) 116134, https://doi.org/10.1016/j.envpol.2020.116134.
[34] L. Yang, N. Li, Y. Kang, J. Liu, Y. Wang, H. Sun, T. Ao, W. Chen, Selenium alleviates toxicity in *Amaranthus hypochondriacus* by modulating the synthesis of thiol compounds and the subcellular distribution of cadmium, Chemosphere 291 (2022) 133108, https://doi.org/10.1016/j.chemosphere.2021.133108.
[35] A.P. Castellanos-Arevalo, A.A. Estrada-Luna, J.L. Cabrera-Ponce, E. Valencia-Lozano, H. Herrera-Ubaldo, S. de Folter, A. Blanco-Labra, J.P. Delano-Frier, *Agrobacterium rhizogenes*-mediated transformation of grain (*Amaranthus hypochondriacus*) and leafy (*A. hybridus*) amaranths, Plant Cell Rep. 39 (2020) 1143–1160, https://doi.org/10.1007/s00299-020-02553-9.
[36] G.H. Han, R.N. Huang, L.H. Hong, J.X. Xu, Y.G. Hong, Y.H. Wu, W.W. Chen, The transcription factor NAC102 confers cadmium tolerance by regulating *WAKL11*

expression and cell wall pectin metabolism in *Arabidopsis*, J. Integr. Plant Biol. 65 (2023) 2262–2278, https://doi.org/10.1111/jipb.13557.
[37] J.J. Yuan, Y.N. Zhao, S.H. Yu, Y. Sun, G.X. Li, J.Y. Yan, J.M. Xu, W.N. Ding, M. Benhamed, R.L. Qiu, C.W. Jin, S.J. Zheng, Z.J. Ding, The *Arabidopsis* receptor-like kinase WAKL4 limits cadmium uptake via phosphorylation and degradation of NRAMP1 transporter, Nat. Commun. 15 (2024) 9537, https://doi.org/10.1038/s41467-024-53898-8.
[38] J. Wang, X. Cao, C. Wang, F. Chen, Y. Feng, L. Yue, Z. Wang, B. Xing, Fe-based nanomaterial-induced root nodulation is modulated by flavonoids to improve soybean (*Glycine max*) growth and quality, ACS Nano 16 (2022) 21047–21062, https://doi.org/10.1021/acsnano.2c08753.
[39] S. Ali, A. Mehmood, N. Khan, Uptake, translocation, and consequences of nanomaterials on plant growth and stress adaptation, J. Nanomater. 6677616 (2021), https://doi.org/10.1155/2021/6677616.
[40] X. Cui, P. Mao, S. Sun, R. Huang, Y. Fan, Y. Li, Y. Li, P. Zhuang, Z. Li, Phytoremediation of cadmium contaminated soils by *Amaranthus Hypochondriacus* L.: the effects of soil properties highlighting cation exchange capacity, Chemosphere 283 (2021) 131067, https://doi.org/10.1016/j.chemosphere.2021.131067.
[41] D. Alidoust, A. Isoda, Effect of γFe_2O_3 nanoparticles on photosynthetic characteristic of soybean (*Glycine max* (L.) Merr.): foliar spray versus soil amendment, Acta Physiol. Plant. 35 (2013) 3365–3375, https://doi.org/10.1007/s11738-013-1369-8.
[42] S. Ghasemi, A.H. Khoshgoftarmanesh, M. Afyuni, H. Hadadzadeh, Iron(II)-amino acid chelates alleviate salt-stress induced oxidative damages on tomato grown in nutrient solution culture, Sci. Hortic. 165 (2014) 91–98, https://doi.org/10.1016/j.scienta.2013.10.037.
[43] A. Aslam, Z. Noreen, M. Rashid, M. Aslam, T. Hussain, A. Younas, S. Fiaz, K. A. Attia, A.A. Mohammed, Understanding the role of magnetic (Fe_3O_4) nanoparticle to mitigate cadmium stress in radish (*Raphanus sativus* L.), Bot. Stud. 65 (2024), https://doi.org/10.1186/s40529-024-00420-4.
[44] A. Sebastian, M.N.V. Prasad, Iron- and manganese-assisted cadmium tolerance in *Oryza sativa* L.: lowering of rhizotoxicity next to functional photosynthesis, Planta 241 (2015) 1519–1528, https://doi.org/10.1007/s00425-015-2276-6.
[45] D. Hou, X. Cui, M. Liu, H. Qie, Y. Tang, R. Xu, P. Zhao, W. Leng, N. Luo, H. Luo, A. Lin, W. Wei, W. Yang, T. Zheng, The effects of iron-based nanomaterials (Fe NMs) on plants under stressful environments: machine learning-assisted meta-analysis, J. Environ. Manag. 354 (2024) 120406, https://doi.org/10.1016/j.jenvman.2024.120406.
[46] V. Chunilall, A. Kindness, S.B. Jonnalagadda, Heavy metal uptake by two edible *Amaranthus* herbs grown on soils contaminated with lead, mercury, cadmium, and nickel, J. Environ. Sci. Health Part B Pestic. Food Contam. Agric. Wastes 40 (2005) 375–384, https://doi.org/10.1081/pfc-200045573.
[47] A. Hussain, S. Ali, M. Rizwan, M.Z.U. Rehman, M.F. Qayyum, H. Wang, J. Rinklebe, Responses of wheat (*Triticum aestivum*) plants grown in a Cd contaminated soil to the application of iron oxide nanoparticles, Ecotoxicol. Environ. Saf. 173 (2019) 156–164, https://doi.org/10.1016/j.ecoenv.2019.01.118.
[48] X. Wu, H. Song, C. Guan, Z. Zhang, Boron alleviates cadmium toxicity in *Brassica napus* by promoting the chelation of cadmium onto the root cell wall components, Sci. Total Environ. 728 (2020) 138833, https://doi.org/10.1016/j.scitotenv.2020.138833.
[49] S. Zheng, C. Xu, G. Lv, H. Shuai, Q. Zhang, Q. Zhu, H. Zhu, D. Huang, Foliar zinc reduced cd accumulation in grains by inhibiting cd mobility in the xylem and increasing cd retention ability in roots, Environ. Pollut. 333 (2023) 122046, https://doi.org/10.1016/j.envpol.2023.122046.
[50] C. Shen, H.L. Fu, B.F. Huang, Q. Liao, Y.Y. Huang, Y.B. Wang, Y.T. Wang, J.L. Xin, Physiological and molecular mechanisms of boron in alleviating cadmium toxicity in *Capsicum annuum*, Sci. Total Environ. 903 (2023) 166264, https://doi.org/10.1016/j.scitotenv.2023.166264.
[51] Y.Y. Huang, C. Shen, X.S. Wang, H.L. Fu, B.F. Huang, Y. Li, H. Wen, Y.F. Wang, W. J. Zhou, J.L. Xin, Boron decreases cadmium accumulation in water spinach by enhancing cadmium retention in the root cell walls, Environ. Sci. Pollut. Res. 30 (2023) 101168–101177, https://doi.org/10.1007/s11356-023-29447-z.
[52] L. Tang, B. Mao, Y. Li, Q. Lv, L. Zhang, C. Chen, H. He, W. Wang, X. Zeng, Y. Shao, Y. Pan, Y. Hu, Y. Peng, X. Fu, H. Li, S. Xia, B. Zhao, Knockout of *OsNramp5* using the CRISPR/Cas9 system produces low Cd-accumulating *indica* rice without compromising yield, Sci. Rep. 7 (2017) 14438, https://doi.org/10.1038/s41598-017-14832-9.
[53] W. Liu, C. Huo, L. He, X. Ji, T. Yu, J. Yuan, Z. Zhou, L. Song, Q. Yu, J. Chen, N. Chen, The NtNRAMP1 transporter is involved in cadmium and iron transport in tobacco (*Nicotiana tabacum*), Plant Physiol. Biochem. 173 (2022) 59–67, https://doi.org/10.1016/j.plaphy.2022.01.024.
[54] R. Takahashi, Y. Ishimaru, H. Shimo, K. Bashir, T. Senoura, K. Sugimoto, K. Ono, N. Suzui, N. Kawachi, S. Ishii, Y.G. Yin, S. Fujimaki, M. Yano, N.K. Nishizawa, H. Nakanishi, From laboratory to field: *OsNRAMP5*-knockdown Rice is a promising candidate for cd phytoremediation in paddy fields, PLoS One 9 (2014), https://doi.org/10.1371/journal.pone.0098816.
[55] L. Tan, Y. Zhu, T. Fan, C. Peng, J. Wang, L. Sun, C. Chen, *OsZIP7* functions in xylem loading in roots and inter-vascular transfer in nodes to deliver Zn/cd to grain in rice, Biochem. Biophys. Res. Commun. 512 (2019) 112–118, https://doi.org/10.1016/j.bbrc.2019.03.024.
[56] E. Ali, M.A. Saand, A.R. Khan, J.M. Shah, S. Feng, C. Ming, P. Sun, Genome-wide identification and expression analysis of detoxification efflux carriers (DTX) genes family under abiotic stresses in flax, Physiol. Plant. 171 (2021) 483–501, https://doi.org/10.1111/ppl.13105.
[57] I.U. Khan, J.K. Rono, B.Q. Zhang, X.S. Liu, M.Q. Wang, L.L. Wang, X.C. Wu, X. Chen, H.W. Cao, Z.M. Yang, Identification of novel rice (*Oryza sativa*) HPP and HIPP genes tolerant to heavy metal toxicity, Ecotoxicol. Environ. Saf. 175 (2019) 8–18, https://doi.org/10.1016/j.ecoenv.2019.03.040.
[58] Y.N. Zhao, M.Q. Wang, C. Li, H.W. Cao, J.K. Rono, Z.M. Yang, The metallochaperone OsHIPP56 gene is required for cadmium detoxification in rice crops, Environ. Exp. Bot. 193 (2022), https://doi.org/10.1016/j.envexpbot.2021.104680.
[59] C.W. Qiu, M. Richmond, Y. Ma, S. Zhang, W. Liu, X. Feng, I.M. Ahmed, F. Wu, Melatonin enhances cadmium tolerance in rice *via* long non-coding RNA-mediated modulation of cell wall and photosynthesis, J. Hazard. Mater. 465 (2024) 104680, https://doi.org/10.1016/j.jhazmat.2023.133251.
[60] B.F. Huang, Q. Liao, H.L. Fu, Z.Y. Ye, Y.X. Mao, J.M. Luo, Y.T. Wang, H.W. Yuan, J. L. Xin, Effect of potassium intake on cadmium transporters and root cell wall biosynthesis in sweet potato, Ecotoxicol. Environ. Saf. 250 (2023) 114501, https://doi.org/10.1016/j.ecoenv.2023.114501.
[61] S. Wojas, J. Hennig, S. Plaza, M. Geisler, O. Siemianowski, A. Sklodowska, A. Ruszczynska, E. Bulska, D.M. Antosiewicz, Ectopic expression of *Arabidopsis* ABC transporter MRP7 modifies cadmium root-to-shoot transport and accumulation, Environ. Pollut. 157 (2009) 2781–2789, https://doi.org/10.1016/j.envpol.2009.04.024.
[62] P. Brunetti, L. Zanella, A. De Paolis, D. Di Litta, V. Cecchetti, G. Falasca, M. Barbieri, M.M. Altamura, P. Costantino, M. Cardarelli, Cadmium-inducible expression of the ABC-type transporter *AtABCC3* increases phytochelatin-mediated cadmium tolerance in *Arabidopsis*, J. Exp. Bot. 66 (2015) 3815–3829, https://doi.org/10.1093/jxb/erv185.
[63] A. Jacquart, R. Brayner, J.-M.E.H. Chahine, H.-D. Nguyet-Thanh, Cd^{2+} and Pb^{2+} complexation by glutathione and the phytochelatins, Chem. Biol. Interact. 267 (2017) 2–10, https://doi.org/10.1016/j.cbi.2016.09.002.
[64] Y. Huang, J. Chen, D. Zhang, B. Fang, T. YangJin, J. Zou, Y. Chen, N. Su, J. Cui, Enhanced vacuole compartmentalization of cadmium in root cells contributes to glutathione-induced reduction of cadmium translocation from roots to shoots in pakchoi (*Brassica chinensis* L.), Ecotoxicol. Environ. Saf. 208 (2021) 111616, https://doi.org/10.1016/j.ecoenv.2020.111616.
[65] Q. Xiao, Y. Wang, Q. Lu, H. Wen, B. Han, S. Chen, X. Zheng, R. Lin, Responses of glutathione and phytochelatins biosysthesis in a cadmium accumulator of *Perilla frutescens* (L.) Britt. under cadmium contaminated conditions, Ecotoxicol. Environ. Saf. 201 (2020) 110805, https://doi.org/10.1016/j.ecoenv.2020.110805.
[66] B. Zhang, Y. Gao, L. Zhang, Y. Zhou, The plant cell wall: biosynthesis, construction, and functions, J. Integr. Plant Biol. 63 (2021) 251–272, https://doi.org/10.1111/jipb.13055.
[67] Y. Xiao, D. Liu, L. Li, Z. Zhang, J.-S. Luo, Cadmium adsorption in leaf cell walls prevents redistribution to silique in *Arabidopsis thaliana* ecotypes Jm-1 and Kyo-0, Environ. Exp. Bot. 194 (2022) 104690, https://doi.org/10.1016/j.envexpbot.2021.104690.
[68] A. Gutsch, S. Zouaghi, J. Renaut, A. Cuypers, J.-F. Hausman, K. Sergeant, Changes in the proteome of *Medicago sativa* leaves in response to long-term cadmium exposure using a cell-wall targeted approach, Int. J. Mol. Sci. 19 (2018) 2498, https://doi.org/10.3390/ijms19092498.
[69] J.S. Peng, Y.J. Wang, G. Ding, H.L. Ma, Y.J. Zhang, J.M. Gong, A pivotal role of cell wall in cadmium accumulation in the Crassulaceae hyperaccumulator *Sedum plumbizincicola*, Mol. Plant 10 (2017) 771–774, https://doi.org/10.1016/j.molp.2016.12.007.
[70] A. Finger-Teixeira, M.D.L. Lucio Ferrarese, A.R. Soares, D. da Silva, O. Ferrarese-Filho, Cadmium-induced lignification restricts soybean root growth, Ecotoxicol. Environ. Saf. 73 (2010) 1959–1964, https://doi.org/10.1016/j.ecoenv.2010.08.021.
[71] M. Yu, R. Zhuo, Z. Lu, S. Li, J. Chen, Y. Wang, J. Li, X. Han, Molecular insights into lignin biosynthesis on cadmium tolerance: morphology, transcriptome and proteome profiling in *Salix matsudana*, J. Hazard. Mater. 441 (2023) 129909, https://doi.org/10.1016/j.jhazmat.2022.129909.
[72] J.A. Verica, Z.H. He, The cell wall-associated kinase (*WAK*) and *WAK*-like kinase gene family, Plant Physiol. 129 (2002) 455–459, https://doi.org/10.1104/pp.011028.
[73] W. Hu, Y. Lv, W. Lei, X. Li, Y. Chen, L. Zheng, Y. Xia, Z. Shen, Cloning and characterization of the *Oryza sativa* wall-associated kinase gene *OsWAK11* and its transcriptional response to abiotic stresses, Plant Soil 384 (2014) 335–346, https://doi.org/10.1007/s11104-014-2204-8.
[74] M. Sivaguru, B. Ezaki, Z.H. He, H.Y. Tong, H. Osawa, F. Baluska, D. Volkmann, H. Matsumoto, Aluminum-induced gene expression and protein localization of a cell wall-associated receptor kinase in Arabidopsis, Plant Physiol. 132 (2003) 2256–2266, https://doi.org/10.1104/pp.103.022129.
[75] X.W. Hou, H.Y. Tong, J. Selby, J. DeWitt, X.X. Peng, Z.H. He, Involvement of a cell wall-associated kinase, WAKL4, in Arabidopsis mineral responses, Plant Physiol. 139 (2005) 1704–1716, https://doi.org/10.1104/pp.105.066910.
[76] H.Q. Lou, W. Fan, J.F. Jin, J.M. Xu, W.W. Chen, J.L. Yang, S.J. Zheng, A NAC-type transcription factor confers aluminium resistance by regulating cell wall-associated receptor kinase 1 and cell wall pectin, Plant Cell Environ. 43 (2020) 463–478, https://doi.org/10.1111/pce.13676.
[77] X. Wu, H. Song, C. Guan, Z. Zhang, Boron mitigates cadmium toxicity to rapeseed (*Brassica napus*) shoots by relieving oxidative stress and enhancing cadmium

chelation onto cell walls, Environ. Pollut. 263 (2020) 114546, https://doi.org/10.1016/j.envpol.2020.114546.
[78] C. Lei, Y. Sun, D.C.W. Tsang, D. Lin, Environmental transformations and ecological effects of iron-based nanoparticles, Environ. Pollut. 232 (2018) 10–30, https://doi.org/10.1016/j.envpol.2017.09.052.
[79] M.S. McKee, J. Filser, Impacts of metal-based engineered nanomaterials on soil communities, Environ. Sci. Nano 3 (2016) 506–533, https://doi.org/10.1039/C6EN00007J.